



RESEARCH PAPER

Intranasal administration of a stapled relaxin-3 mimetic has anxiolytic- and antidepressant-like activity in rats

Subhi Marwari^{1,2}  | Anders Poulsen³ | Norrapat Shih⁴ | Rajamani Lakshminarayanan^{5,6} | R. Manjunatha Kini⁴ | Charles William Johannes⁷ | Brian William Dymock² | Gavin Stewart Dawe^{1,8} 

¹Department of Pharmacology, Yong Loo Lin School of Medicine, National University of Singapore, Singapore

²Department of Pharmacy, Faculty of Science, National University of Singapore, Singapore

³Department of Medicinal Chemistry, Experimental Therapeutics Centre, Agency for Science, Technology and Research (A*STAR), Singapore

⁴Department of Biological Sciences, Faculty of Science, National University of Singapore, Singapore

⁵Anti-Infectives Research Group, Singapore Eye Research Institute, Singapore

⁶Ophthalmology and Visual Sciences Academic Clinical Program, Duke-NUS Medical School, Singapore

⁷Institute of Chemical and Engineering Sciences, Agency for Science, Technology and Research (A*STAR), Singapore

⁸Neurobiology and Ageing Programme, Life Sciences Institute, National University of Singapore, Singapore

Correspondence

Subhi Marwari and Gavin S. Dawe,
Department of Pharmacology, Yong Loo Lin
School of Medicine, MD3, #04-01, 16 Medical
Drive, National University of Singapore,
Singapore.
Email: gavindawe@nus.edu.sg; a0135981@u.
nus.edu

Funding information

Ministry of Education, Singapore, Academic
Research Fund Tier 1, Grant/Award Numbers:
T1-NUHS O-CRG 2016 Oct-18 and T1-BSRG
2014-03; NMRC NUHS Centre Grant—Neu-
rosience Phenotyping Core, Grant/Award
Number: NMRC/CG/M009/2017_NUH/
NUHS NMRC/CG/013/2013

Background and Purpose: Depression and anxiety are common causes of disability, and innovative tools and potential pharmacological targets are actively sought for prevention and treatment. Therapeutic strategies targeting the relaxin-3 peptide or its primary endogenous receptor, RXFP3, for the treatment of major depression and anxiety disorders have been limited by a lack of compounds with drug-like properties. We proposed that a hydrocarbon-stapled mimetic of relaxin-3, when administered intranasally, might be uniquely applicable to the treatment of these disorders.

Experimental Approach: We designed a series of hydrocarbon-stapled relaxin-3 mimetics and identified the most potent compound using in vitro receptor binding and activation assays. Further, we assessed the effect of intranasal delivery of relaxin-3 and the lead stapled mimetic in rat models of anxiety and depression.

Key Results: We developed an *i,i+7* stapled relaxin-3 mimetic that manifested a stabilized α -helical structure, proteolytic resistance, and confirmed agonist activity in receptor binding and activation in vitro assays. The stapled peptide agonist enhanced food intake after intracerebral infusion in rats, confirming in vivo activity. We showed that intranasal delivery of the lead *i,i+7* stapled peptide or relaxin-3 had orexigenic effects in rats, indicating a potential clinically translatable route of delivery. Further, intranasal administration of the lead *i,i+7* stapled peptide exerted

Abbreviations: CD, circular dichroism; CRH, corticotrophin-releasing hormone; EZM, elevated zero maze; H3, human relaxin-3 peptide; LDB, light-dark box; NI, nucleus incertus; NSFT, novelty-induced suppression of feeding test; PVN, paraventricular nucleus; RXFP, relaxin family peptide receptor; SSRI, selective serotonin reuptake inhibitor

This is an open access article under the terms of the Creative Commons Attribution-NonCommercial License, which permits use, distribution and reproduction in any medium, provided the original work is properly cited and is not used for commercial purposes.

© 2019 The Authors. British Journal of Pharmacology published by John Wiley & Sons Ltd on behalf of British Pharmacological Society.

anxiolytic and antidepressant-like activity in anxiety- and depression-related behaviour paradigms.

Conclusions and Implications: Our preclinical findings demonstrate that targeting the relaxin-3/RXFP3 receptor system via intranasal delivery of an *i,i+7* stapled relaxin-3 mimetic may represent an effective treatment approach for depression, anxiety, and related neuropsychiatric disorders.

1 | INTRODUCTION

Medical need to improve upon the limited effectiveness and undesirable side effects of existing therapeutic agents drives the quest for novel drug candidates for neuropsychiatric disorders. Together, major depression and anxiety disorders markedly contribute to the global prevalence of disease worldwide (Grupe & Nitschke, 2013; Kessler et al., 2009; Wang & Insel, 2010). The Global Burden of Diseases, Injuries, and Risk Factors Study 2010 data revealed that mental and substance abuse disorders account for 7.4% of the global burden of disease, with major depressive disorders alone representing 40% and anxiety disorders contributing 14.6% of this burden (Whiteford et al., 2013; Whiteford & Baxter, 2013). Over the past two decades, success with new drugs for neuropsychiatric disorders has been scarce, and the strategies for targeting these disorders have primarily been based on conventional, rather than novel, approaches.

Neuropeptide receptors have become one of the most attractive therapeutic targets for treatment of neuropsychiatric disorders due to accelerated advancement in understanding of the structure of peptide receptor ligands and their efficient synthesis (Belzung, Yalcin, Griebel, Surget, & Leman, 2006). The neuropeptide **relaxin-3** (insulin-like 7) belongs to the insulin superfamily (Burazin et al., 2002), and the native receptor for relaxin-3 is relaxin family peptide receptor 3 (**RXFP3**), which was first identified as an orphan GPCR 135 (Liu et al., 2003). Relaxin-3 is abundantly expressed in **GABA**-expressing projection neurons in the brainstem nucleus incertus (NI) and in smaller groups of neurons in the pontine raphe, periaqueductal grey, and dorsal to the substantia nigra (Ma et al., 2007; Tanaka et al., 2005). Relaxin-3 mediates its effects by modulating its cognate receptor RXFP3 in the mammalian brain (Liu et al., 2003; Matsumoto et al., 2000). The dense projection of relaxin-3 immunoreactive fibres and broad distribution of RXFP3 mRNA/binding sites in the septum, hypothalamic, and hippocampal regions of the rodent and primate brain (Ma, Sang, Lanciego, & Gundlach, 2009) suggests that endogenous relaxin-3/RXFP3 receptor signalling act as an “arousal” neurotransmitter system that can modulate a variety of behavioural outputs, such as the regulation of appetite and stress-related responses, and alter hippocampal θ rhythms and associated spatial memory (Ganella, Ryan, Bathgate, & Gundlach, 2012). The wide distribution of relaxin-3/GABA innervations across the brain made by the relaxin-3/RXFP3 system shows remarkable parallels with the serotonergic raphe (Lesch & Waider, 2012; Monti & Jantos, 2008) and noradrenergic locus coeruleus pathways (Berridge, Schmeichel, & Espana, 2012; Takagi,

What is already known

- Relaxin-3 and its receptor are a therapeutic target for the treatment of neurological disorders.
- Complex relaxin-3 synthesis and requirement for central administration have hindered translational potential.

What this study adds

- Discovery of a lead hydrocarbon-stapled mimetic establishes a compelling alternative with simplified synthesis and potency.
- Combining lead peptide with clinically viable intranasal delivery unleashes the relaxin-3/RXFP3 systems' anxiolytic and antidepressant potential.

What is the clinical significance

- The current study presents a practical treatment approach for targeted clinical translation.
- Further clinical research can examine connection of relaxin-3 signalling with metabolic and psychiatric disorders.

Shiosaka, Tohyama, Senba, & Sakanaka, 1980) and is likely to contribute to the central stress responses involved in the pathophysiology of anxiety and depression (Smith et al., 2010). Further, it has been reported that RXFP3 receptor expression is high within the paraventricular nucleus (PVN) of the hypothalamus (Kania et al., 2017). Intracerebroventricular injection of relaxin-3 in rodents elevated **corticotrophin-releasing hormone** (CRH) and *c-fos* mRNA within the PVN and increased the plasma levels of **adrenocorticotrophic hormone** (Watanabe, Miyamoto, Matsuda, & Tanaka, 2011). These findings are indicative of activation of the hypothalamic-pituitary-adrenal axis and suggest that the gross effect of behavioural responses following global activation of RXFP receptors is anxiolytic/antidepressant (Nakazawa et al., 2013; Ryan et al., 2013). Therefore, it is of interest to develop RXFP3 receptor ligands as tools to explore the potential of targeting the relaxin-3/RXFP3 receptor system for treatment of anxiety and depression.

Hydrocarbon stapling of **relaxin-3 B-chain** derived peptides has emerged as a viable strategy to produce small peptide agonists for RXFP3 receptors (Hojo et al., 2016; Jayakody et al., 2016). Peptide

stapling is a macrocyclization strategy, achieved by ring-closing olefin metathesis through incorporation of non-natural α -substituted amino acids at positions spanning one ($i,i+4$) or two ($i,i+7$) turns of the α -helix to effectively cross-link the residues. These all-hydrocarbon constraining staples can confer an α -helical structure and improve biological activity and proteolytic stability by reproducing the bioactive structure. In the current study, we investigated the utility of different relaxin-3 B-chain hydrocarbon stapling chemistries in helical induction and biological activity. A high-affinity $i,i+7$ hydrocarbon-stapled ligand (14s21) provided a molecular tool for exploring the pharmacological potential of the relaxin-3/RXFP3 receptor system. Because drug delivery is a potential problem in peptide therapeutics, to explore the prospects of advancing this novel ligand system towards translatable therapeutic applications, we examined whether intranasal delivery could provide an approach to deliver the peptide into the brain and produce the same behavioural effects seen with direct central administration in rodents. Here, we report the strategic development of a lead relaxin-3/ receptor system stapled peptide agonist combined with the first successful approach for intranasal delivery of relaxin-3 or the 14s21 ($i,i+7$) stapled peptide to achieve anxiolytic and antidepressant-like activity in animal models.

2 | METHODS

2.1 | Design of stapled peptides and variants

We designed a series of stapled peptides using *in silico* modelling and a comprehensive staple scanning approach to derive optimized stapled peptides and variants for testing. We used previously reported structure–activity relationships of human relaxin-3 peptide (H3) relaxin to generate a molecular model (Bathgate et al., 2013; Hu et al., 2016). Structure–activity studies on relaxin-3 have identified the key residues involved in binding and activation of the RXFP3 receptor, including ArgB12, IleB15, ArgB16, and PheB20 located in the B-chain helical region and the two C-terminal residues ArgB26 and TrpB27 at the end of a flexible tail, which are reported to be critical for receptor activation (Kuei et al., 2007). Stapling sites were chosen so that they did not interfere with the residues critical for binding and activation of the RXFP3 receptor. Based on this knowledge and with *in silico* modelling predictions, we designed stapled peptides that were stapled at $i,i+4$ [18th and 22nd positions (18s22) and 14th and 18th positions (14s18)] positions and $i,i+7$ [11th and 18th positions (11s18) and 14th and 21st positions (14s21)] positions. Based on our previous published results on $i,i+4$ stapled peptides (Jayakody et al., 2016), it was evident that stapling at more central positions stabilizes the α -helix, and thus, in our current study, we also synthesized the lactam and disulfide variant of the previously published ($i,i+4$) 14s18 stapled peptide. To study the effective minimized active structure of relaxin-3 B-chain stapled peptide, we also attempted to truncate the seven residues from the N-terminus of the relaxin-3 B-chain [R3B8-27 (14s18)-14s18]. We compared the binding affinity and activation profile of the truncated (14s18) peptide with those of the full-length [R3B (14s18)] 14s18

TABLE 1 Stapled H3 B-chain analogues synthesized and characterized in the current study

| Peptide # | Analogue | Sequence |
|-----------|-----------------|----------------------------------|
| 1 | H3 B-chain | RAAPYGVRLSGREFIRAVIFTSGGSRW |
| 2 | 14s18 | RAAPYGVRLSGRE-S5IRA-S5IFTSGGSRW |
| 3 | 18s22 | RAAPYGVRLSGREFIRA-S5IFT-S5GGSRW |
| 4 | 14s18 | RLSGRE-S5IRA-S5IFTSGGSRW |
| 5 | 13s17 | RLSGR-S5FIR-S5VIFTSGGSRW |
| 6 | H3 B-chain | RLSGREFIRAVIFTSGGSRW |
| 7 | 14s18-Lactam | RAAPYGVRLSGRE-KIRA-DIFTSGGSRW |
| 8 | 14s18-Disulfide | RAAPYGVRLSGRE-CIRA-CIFTSGGSRW |
| 9 | 14s21 | RAAPYGVRLCGRE-R5IRAVIF-CGGSRW |
| 10 | 14s21-Ser | RAAPYGVRLSGRE-R5IRAVIF-S8SGGSRW |
| 11 | 11s18 | RAAPYGVRLC-R5REFIRA-S8IFTCCGGSRW |

Abbreviations: **S5**, (S)-2-(4-pentenyl) alanine; **R5**, (R)-2-(4'-pentenyl) alanine; **S8**, (S)-2-(7'-octenyl) alanine.

stapled peptide. Further, we compared the 14s18 peptide with the previously reported high-affinity agonist 13s17 stapled peptide [R3B8-27 (13s17); Hojo et al., 2016; Table 1].

2.2 | Molecular modelling

The NMR structure of relaxin-3 (PDB entry 2FHW; Rosengren et al., 2006) was prepared using Protein Preparation Wizard in Maestro version 10.3 (Maestro, RRID:SCR_016748). All the peptides, including the wild-type relaxin-3, relaxin-3 B-chain, and stapled peptide variants, were investigated as described previously (Jayakody et al., 2016).

2.3 | Peptide synthesis and characterization

Hydrocarbon-stapled peptides and variants were purchased from Biosynthesis Inc., USA. Staples were incorporated by placing the eight-carbon metathesized cross link in (S)-configuration at the $i(14)$, $i+4(18)$, and $i(18)$, $i+4(22)$ positions with (S)-2-(4'-pentenyl)alanine (S_5). Lactam bond formation was undertaken at the 14(i) and 18($i+4$) positions by replacing the residues with K (Lys) and D (Asp). Disulfide bond formation was induced by replacing the residues at the 14(i) and 18($i+4$) positions with C (Cys). Hydrocarbon stapling for $i,i+7$ peptides was carried out with an 11-carbon cross link using a combination of R-2-(4'-pentenyl) alanine (R_5) and S-2-(7'-octenyl) alanine (S_8) at the $i,i+7$ positions for the 14s21 and 11s18 stapled peptides. Peptides were purified by the manufacturer using HPLC to >95% purity. We further verified the molecular weight and purity of the peptides via MS and RP-HPLC analysis (refer to Table S1 for analytical data and mass profiles of the synthesized peptides).

2.4 | Circular dichroism spectroscopy

The solution conformation properties of the peptides were evaluated using circular dichroism (CD) spectroscopy on a JASCO J-815 spectrometer (Tokyo, Japan). All peptide samples were measured in water, and the spectra generated were an average of three independent scans. The mean α -helical content of each peptide was calculated using the mean residual ellipticity at 222 nm as previously described (Jayakody et al., 2016).

2.5 | Cell lines and culture

HEK293T cells stably expressing RXFP3 receptors (HEK-RXFP3) were provided by Prof. Roger Summers (Monash Institute of Pharmaceutical Sciences and Department of Pharmacology, Monash University). HEK-RXFP3 cells were maintained in 75-cm² flasks at 37°C in a humidified atmosphere in DMEM. DMEM was supplemented with 10% (v/v) FBS and 1X penicillin/streptomycin (10,000 U·ml⁻¹). Cells were harvested at 90% confluency for plating onto PLL-precoated well plates for receptor-ligand binding and receptor activation assays.

2.6 | Eu(III)-based ligand binding assay

The receptor binding affinity of the peptides was measured using HEK293T cells stably expressing RXFP3 receptors. The competition binding assays were carried out as described previously (Haugaard-Kedstrom, Wong, Bathgate, & Rosengren, 2015; Jayakody et al., 2016). Briefly, variable concentrations of non-labelled R3B1-22R, H3 relaxin, H3 relaxin B-chain, and stapled peptides and variants (1 pM to 100 μ M) and a fixed concentration of Eu-DTPA-R3B1-22R (8 nM) were utilized in an otherwise identical procedure and under the conditions provided above. The europium binding curves were fitted to a one-site competition curve, and the pK_i values are expressed as the mean \pm SEM of at least three independent experiments, with triplicate determinations within each assay.

2.7 | Inhibition of cAMP accumulation assay

The peptides were tested for their ability to inhibit cAMP activity in HEK-RXFP3 cells using an assay previously described (Harris, Creason, Brulte, & Herr, 2012; Jayakody et al., 2016). Briefly, the cells were treated with the relaxin-3 peptides in triplicate at different concentrations (0.1 pM to 10 μ M) for 5 min and then with forskolin (5 μ M) for 15 min in a 37°C incubator. Cells were lysed by shaking with 50 μ l 0.1-M HCl for 20 min, after which they were scraped and centrifuged at 1,000 g for 10 min. Next, 50 μ l of supernatant was applied on plates precoated with mouse anti-rabbit IgG and assayed according to the manufacturer's instructions (cAMP EIA Kit, Cayman Chemicals, Ann Arbor, MI). The cAMP level is expressed as a percentage of the forskolin-induced response. The concentration-response data were analysed via non-linear fitting and estimation of pEC₅₀ in GraphPad Prism.

2.8 | ERK1/2 phosphorylation assay

Estimation of the level of phosphorylated ERK was performed using a western blot-based technique as previously described (Shaul & Seger, 2006). Cells were plated into 12-well plates with complete DMEM and then serum starved for 4 hr before experimentation and assayed for phospho-ERK1/2. Cells were treated with H3 relaxin and varying concentrations of 14s21 stapled peptide (1 pM to 100 μ M) for 5 min. After the reaction, the cells were immediately lysed with 2X SDS loading buffer. Cell lysate was boiled at 100°C for 10 min and separated by electrophoresis through 8% SDS-polyacrylamide gels for 2 hr at 100 V. After this, proteins were transferred to a PVDF membrane for 75 min at 110 V, followed by blocking with 5% blocking solution in TBS/Tween 20, and immunoblotted for total ERK (tERK1/2) using an anti-p44/p42 MAPK (ERK1/2) antibody (Cell Signaling Technology Cat# 4695, RRID:AB_390779) diluted 1:1,000 in 1% BSA in TBS/Tween 20 and goat anti-rabbit HRP-conjugated IgG secondary antibody (Thermo Fisher Scientific Cat# 31460, RRID:AB_228341) diluted 1:5,000. Protein bands were visualized via chemiluminescence using Luminata Forte Western HRP substrate (Merck Millipore, Billerica, MA, USA). After visualization, primary and secondary antibodies were stripped using Restore western blot stripping buffer (Thermo Fischer Scientific, Rockford, USA), and the blots were re-probed with anti-phospho-p44/p42 MAPK (ERK1/2) antibody (Cell Signaling Technology Cat# 4370, RRID:AB_2315112) diluted 1:1,000 and visualized as described above. The density of phospho-ERK1/2 and total ERK1/2 was determined using ImageJ software (ImageJ, RRID:SCR_003070), and the density of phospho-ERK1/2 was normalized to that of total ERK1/2. Normalization was required to calculate the phosphorylated ERK1/2 expression relative to the total ERK1/2 expression to control for loading variance.

2.9 | Thermal stability assay

Temperature-dependent CD spectra of each peptide (50–65 μ M) were recorded at varying temperatures (every 5°C from 20°C to 90°C) from 190 to 260 nm. The spectra presented are an average of three independent scans with a scan speed of 20 nm·min⁻¹. Replicate measurements as a function of temperature reproduced the spectra within \pm 5% after the heating cycle. To obtain the melting temperatures, we analysed the thermal unfolding curves using a two-state model with a 95% confidence interval as previously described (Jayakody et al., 2016).

2.10 | Protease resistance assay and LC-MS/MS analysis

Peptides (3 mg·ml⁻¹) were digested with trypsin (1 mg·ml⁻¹) in water to prepare peptide solution; 25 μ l of digestion mixture was taken at each time point (0, 1, 3, 5, 7, 9, and 25 hr), and then, the amount of intact peptide was quantified via serial injection over time. The digested products were quantified using LC/MS-based peak detection

at 220 nm. Each experiment was performed in triplicate. A plot of the per cent fraction of intact peptide versus time yielded an exponential decay curve, and half-lives were determined by non-linear regression analysis using GraphPad Prism software. LC-MS analysis was performed on a Thermo Scientific LCQ Fleet ion trap mass spectrometer coupled to a Thermo Scientific Accela 600 HPLC pump (Waltham, MA, USA). Chromatographic separation was performed using an Accucore RP-MS column (2.1 × 100 mm; 2.6 μm), and column temperature was maintained at 40°C. Gradient separation was performed using a mixture of 0.1% formic acid and acetonitrile in 0.1% formic acid. MS was conducted on a Thermo Scientific LCQ Fleet ion trap mass spectrometer with an electrospray ionization interface in positive ion mode. An LC-MS method with scan range 50–2000 m/z was used for detection of the peptides. Peptides were quantified via extracted-ion chromatography and peak area analysis using Thermo Xcalibur software (Thermo Xcalibur, RRID:SCR_014593). The following mass ranges were used for extracted-ion chromatography: 600.3–606.3 m/z for the R3 B-chain, 751.8–757.8 m/z for 14s18, and 769.97–775.97 m/z for 14s21. Source parameters were as follows: sheath gas flow rate 30 L·min⁻¹; auxiliary gas flow rate 5 L·min⁻¹; spray voltage 4.5 kV; capillary temperature 350°C; capillary voltage 40 V; and tube lens 95 V. LC-MS grade acetonitrile and the Accucore RP-MS column were from Thermo Scientific (Waltham, MA, USA). LC-MS grade formic acid was from Sigma-Aldrich (St. Louis, MO, USA).

2.11 | Ethical statement

All animal care and experimental procedures were approved by the Institutional Animal Care and Use Committee of the National University of Singapore. The procedures conducted followed the guidelines of the National Advisory Committee for Laboratory Animal Research, Singapore, and were in accordance with the Guide for the Care and Use of Laboratory Animals, National Research Council of the National Academies, USA. Animal studies are reported in compliance with the ARRIVE guidelines (Kilkenny, Browne, Cuthill, Emerson, & Altman, 2010) and with the recommendations made by the *British Journal of Pharmacology*.

2.12 | Compliance with requirements for studies using animals

Because rats have been widely used in previous investigations of relaxin-3 and relaxin-3 B-chain peptides (see Kumar et al., 2017; Ma, Smith, Blasiak, & Gundlach, 2017), rats were used to allow comparison of the current results with the previous literature. Rats were also appropriate because they have been widely used in translational pharmacological research on anxiety, depression, and other neuropsychiatric disorders (Lezak, Missig, & Carlezon, 2017; Pollak, Rey, & Monje, 2010). To allow comparison with previous intracerebroventricular administration studies (Albert-Gasco et al., 2017; McGowan et al., 2006), male rats were used for the current intracerebroventricular administration experiments. Consequently, to allow comparison

between our intracerebroventricular administration results and our intranasal administration results, male rats were used for the subsequent intranasal administration experiment. As sex-specific differences in food intake have been reported following central administration of relaxin-3 in rats (Calvez, de Avila, & Timofeeva, 2017), we compared intranasal administration in male and female rats. We found no significant difference between male and female rats (Figure 4d). Female rats are reported to be no more variable than male rats across diverse traits relevant to neuroscience studies (Becker, Prendergast, & Liang, 2016), and female rats have been used for studies involving intranasal administration (Derkach, Bondareva, Chistyakova, Berstein, & Shpakov, 2015; Kumar et al., 2018). Thus, we used female rats for the subsequent intranasal administration studies.

Experimentally naive male Sprague-Dawley (SD) rats ($n = 44$, InVivos Pte Ltd), weighing 200–230 g at the time of arrival (for intracerebroventricular administration) or 150–180 g (for intranasal administration), and female SD rats (InVivos Pte Ltd), weighing 120–150 g ($n = 68$, for intranasal administration), were utilized in this study. The female rats were separated into three cohorts. One cohort of female SD rats was used for the intranasal administration dose-response optimization studies ($n = 22$). A second cohort of female SD rats ($n = 24$) was used for the elevated zero maze (EZM), light-dark box (LDB), open field test, and novelty-induced suppression of feeding tests (NSFTs). A third cohort of female rats ($n = 22$) was used for the repeat forced-swim test (FST) experiment. Rats that (a) lost the cannula before the behavioural testing was completed [N (excluded) = 6, (2 vehicle, 2 H3, and 2 14s21)], (b) did not take the doses during the stipulated time of intranasal dosing [N (excluded) = 6 (male: 1 H3, 1 vehicle; and female: 1 vehicle, 1 H3, and 2 14s21)], or (c) did not complete the behavioural testing [Cohort-2, N (excluded) = 3 (1 vehicle, 2 14s21); Cohort-3, N (excluded) = 2 (1 vehicle, 1 14s21)] were excluded from the study. Rats were housed in individually ventilated cages with corn cob bedding and fed standard irradiated rodent chow (TEKLAD irradiated global 18% protein rodent diet 2918, 18% calories from fat; Envigo, Madison WI, USA) and water ad libitum. For the intracerebroventricular administration experiment, single housing was required after intracerebroventricular cannula implantation to eliminate the risk of cage mates interfering with the intracranial implant. Therefore, to allow comparison with the intracerebroventricular administration experiments, the subsequent intranasal administration experiments had to be conducted in singly housed animals. Moreover, while monitoring feeding and drinking and when using the Laboratory Animal Behaviour Observation Registration and Analysis system (LABORAS, Metris, Netherlands) to monitor behaviour, single housing was experimentally necessary to obtain accurate results. All singly housed rats were provided a Nylabone (Nylabone Products, Neptune City, NJ, USA) as enrichment. Although housed in individually ventilated cages, rats also had auditory and visual stimulus from surrounding cages. For the intracerebroventricular administration experiment, the animals (for intracerebroventricular studies) were initially housed in pairs in individually ventilated cages. For the intranasal administration experiments, the animals were acclimated for 14 days, two per

cage, and then randomly assigned to the experimental groups and housed one per cage. Body weight was monitored during the experimental procedures. The animal colony was maintained at $22 \pm 2^\circ\text{C}$ during a 12-hr light/12-hr dark cycle with light on from 7:00 a.m. to 7:00 p.m. All behavioural testing occurred during the light phase between 8:00 a.m. and 1:00 p.m.

2.13 | Stereotaxic implantation of cannulas into the lateral ventricle

Following the acclimatization period, the rats were first anaesthetized with a cocktail of ketamine ($75 \text{ mg}\cdot\text{kg}^{-1}$) and xylazine ($10 \text{ mg}\cdot\text{kg}^{-1}$) injected intraperitoneally and then mounted onto a stereotaxic frame. The scalp was shaved and thoroughly disinfected with iodine solution and ethanol. After a midline sagittal incision was made, the skull was cleaned, and burr holes were drilled in the skull at the coordinates corresponding to the lateral ventricle. A guide cannula (Plastics One, USA) was unilaterally implanted using the following coordinates relative to the bregma (flat skull): AP, -0.8 mm ; ML, -1.4 mm ; and DV, -3.6 mm (Paxinos & Watson, 2007). One screw mounted in the skull and covered with dental cement served as an anchor for the guide cannula. The scalp was sutured and cleaned with iodine solution to prevent infection. A dust cap was inserted into the guide cannula to prevent blockage when not in use. The rats were then single housed and allowed a rehabilitation period of 1 week, with carprofen ($5 \text{ mg}\cdot\text{kg}^{-1}$) and enrofloxacin ($10 \text{ mg}\cdot\text{kg}^{-1}$) treatments injected subcutaneously for the first 5 days, during which they were handled and weighed daily to habituate them to the experimenter. A stylet of stainless-steel wire was inserted into each cannula to maintain patency. Correct positioning of the cannula was verified by injecting $5 \mu\text{l}$ of a $4 \text{ ng}\cdot\mu\text{L}^{-1}$ angiotensin II solution and observing a positive dipsogenic response, defined as repeated drinking episodes of $>5 \text{ s}$ that commenced within 1 min of angiotensin II administration (McGowan et al., 2005). Only animals with correct cannula placement were included in the data analysis. Similar surgical procedures targeted at the NI were also established in our lab and conducted in previous studies (Kumar et al., 2015). The rats were individually placed in LABORAS home cages, and behavioural parameters such as locomotion, velocity, distance travelled, eating, drinking, rearing, and grooming were then continuously assessed for 4 hr by the LABORAS software.

2.14 | Drug infusion procedure in SD rats after intracerebroventricular surgery

Relaxin-3 ($100 \text{ pmol}/5 \mu\text{l}$; i.e., $0.5 \mu\text{g}/5 \mu\text{l}$ or $1 \text{ nmol}/5 \mu\text{l}$; i.e., $5 \mu\text{g}/5 \mu\text{l}$), 14s21 stapled peptide ($1 \text{ nmol}/5 \mu\text{l}$; i.e., $3 \mu\text{g}/5 \mu\text{l}$), or vehicle (equivalent amount of sterile isotonic saline) was infused into the lateral ventricle over a period of 30 s. All solutions were infused in a $5\text{-}\mu\text{l}$ volume and administered using an infusion cannula connected by polyethylene tubing to a $10\text{-}\mu\text{l}$ Hamilton microsyringe. The peptide administered through the infusion cannula was left in place for 1 min before recapping of the cannula and placement of the rats in the

LABORAS cages for the experimental trial. Animals were immediately placed into the cages (containing no bedding) after drug infusion for 4 hr. Food crumbs detected on the floor of the apparatus were included in the determination of food weights. Data were recorded (a) by manual food and water intake measurement after every 1 hr and (b) by the LABORAS software, and 4 hr of data were processed and extracted in 10-min-sized bins and exported and tabulated in Microsoft Excel (RRID:SCR_016137). Thereafter, statistical analysis was carried out using GraphPad Prism 7 software. Statistical significance was routinely calculated for the behaviour of (relaxin-3 + saline)/(14s21 stapled peptide + saline)/(relaxin-3 + 14s21 stapled peptide) the grouped animals in LABORAS cages.

2.15 | LABORAS optimization and feeding assays

The rats were individually placed in LABORAS home cages, which were similar to the regular home cages in which they were housed. Behavioural parameters, such as locomotion, velocity, distance travelled, eating, drinking, rearing, and grooming, were then continuously assessed for 4 hr by the LABORAS software. A food hopper and drinking water bottle were located on opposite walls of the cage. The rats were initially habituated to the LABORAS cages for 5 days before the test session was applied, and behavioural studies were performed during the light phase beginning at 07:00 hr. All food intake and water consumption measurement experiments were carried out in the individual home cage of each rat. Prior to the start of the experiment, a predetermined amount of standard rat chow (40 gm) was placed on a metal feed rack inside the cage. Water bottles were weighed and placed on each individual cage. Food and water consumed and the weight of rats were measured every morning and recorded. The LABORAS plate was examined to collect any small feed remnants that may have dropped while rats were eating, and these were included in the weighing. Food left in the food hopper was also determined by subtracting the weight of food and water at 1 hr intervals in 4-hr sessions from the initial food weight (i.e., weight of the food at the start of the session). Groups of rats were injected using a crossover design ($n = 6 \text{ rats}/\text{group}$), whereby each rat received peptide and vehicle. The rats were returned to their home cages, and at least 72 to 120 hr passed before the next test to allow the peptide to be excreted.

2.16 | Post-mortem analysis

The rats were anaesthetized with an overdose of pentobarbital, and $0.1 \mu\text{l}$ of pontamine sky blue dye was infused into the lateral ventricle via the guide cannula in the same manner as the drug infusion described above. Subsequently, transcardial perfusion was carried out with isotonic saline followed by 4% paraformaldehyde in phosphate buffer (0.1 M). The brains were subsequently post-fixed in 4% paraformaldehyde at 4°C for 2 days and soaked in 15% sucrose and 30% sucrose at 4°C for 2 days each. Sections ($40 \mu\text{m}$) were collected serially in PBS with a cryostat (CM 3050, Leica Biosystems, Germany).

The sections were then Nissl stained to identify the track of the implanted cannula (Figure 3a-i,a-ii).

2.17 | Intranasal drug administration

For the intranasal dose–response studies, rats received different concentrations of H3 relaxin (2.75, 27.5, 275, or 2,750 $\mu\text{g}\cdot\text{kg}^{-1}$), 14s21 peptide (0.015, 0.15, 1.5, or 15 $\text{mg}\cdot\text{kg}^{-1}$), or sterile isotonic saline. For the highest doses (2,750 $\mu\text{g}\cdot\text{kg}^{-1}$ H3 relaxin and 15 $\text{mg}\cdot\text{kg}^{-1}$ 14s21 peptide), the peptides were dissolved in 20% DMSO and sterile saline. Dose solution aliquots for each experiment were stored at -80°C until the last day of the experiment. Intranasal delivery in SD rats was carried out manually without anaesthesia as previously described (Lukas & Neumann, 2012; Thorne, Pronk, Padmanabhan, & Frey, 2004) with slight modifications. To minimize non-specific stress during the application procedure, each rat was handled (including adapting the animal to the supine position) by the handler for 10 min daily for at least 5 days prior the day of the experiment. Intranasal administration of vehicle was performed in the same way as drug treatment, that is, holding the animal in the supine position. In detail, the head of a conscious rat was restrained in a supine position, and two pads were placed under the dorsal neck to extend the head back towards the supporting surface. All rats were treated with relaxin-3, 14s21 peptide, or saline/vehicle delivered over both nares alternatively using a 100- μl pipette. An average of 50- μl total peptide dose solution divided into 8- to 10- μl drops was administered every 1–2 min by alternating between each naris, over a total of 6.5 to 7 min, until the drugs were naturally sniffed in by the rat (Migliore et al., 2014). The rat was held for an additional 30–60 s to ensure the fluid was inhaled. Rats were then returned to their home cage until behavioural testing started 25–35 min later.

2.18 | Behavioural assessment after intranasal drug administration

All behavioural testing occurred during the light phase between 8:00 a.m. and 1:00 p.m. Before the start of the experiment trial, rats were housed singly and acclimatized to the behaviour room for 1 hr before the experiments. One animal was selected and transferred in a covered box, and intranasal administration of the drug and the behaviour experiment were performed under dim light. The animal remained in the cage for 20 min to allow adequate absorption of the drug and then was placed on the zero maze at a junction between an open and closed arm, facing into the closed area. All testing was conducted under dim lighting conditions. After 5 min, the animal was removed from the maze, and the maze was washed using an ethanol/water solution to avoid olfactory cues transferring from one experimental session to the next. Once testing was completed, computer-based event recording and ethological analysis software (EthoVision XT, RRID:SCR_000441) were used to register and analyse the relevant experimental variables.

2.19 | Elevated zero maze

The design of the zero maze employed was based on that originally proposed by Shepherd, Grewal, Fletcher, Bill, and Dourish (1994). The maze was constructed of black acrylic in a circular track 10 cm wide and 105 cm in diameter that was elevated 65 cm above the floor (San Diego Instruments, San Diego, CA). The maze was divided into four quadrants of equal length, with two opposing open quadrants with 1-cm high clear acrylic curbs to prevent falls and two opposing closed quadrants with black acrylic walls 27 cm in height. A 5-min trial under dim lighting conditions was conducted with the animal placed in the centre of a closed quadrant. The dependent measures were time spent in the open, % open arm entries, close to open arm transitions, and head dips. Time in open arms was defined as the animal having both front legs past the boundary of the closed area extending into an open quadrant.

2.20 | LDB testing

This test was performed to assess anxiety behaviour (Crawley, 1981). The apparatus was a glass box divided into two compartments; one compartment was “light” and the other was “dark” (30 × 30 × 50 cm). A hole in the partition separating the two compartments allowed access between the compartments. This system was based on the internal conflict between approach and avoidance of anxiety-provoking areas (here, the light compartment). At the beginning of the experiment, the rat was placed in the light compartment of the box (440 lux) and was set free to explore it for 5 min. The automated EthoVision XT software tracked the movement of the rat. During this experimental trial, the number of entries into each compartment and the time spent in the illuminated light compartment were recorded. The apparatus was cleaned thoroughly with 70% ethanol and allowed to dry before and between each animal.

2.21 | Open field test

The rats were placed in an open field to evaluate locomotor activity. The open field was a 120-cm diameter circular arena, bordered by a 50-cm-high walls. The central area was defined as the central zone, in which animal activity was regarded as a measure of anxiety. The test was performed as described previously (Grivas, Markou, & Pitsikas, 2013). On the test day, the rats were transported to the dimly illuminated (20 lux) test room and were left undisturbed in their home cage for 1 hr. During each open field test session, the animal was placed on one of the corners facing the wall of the apparatus and set free to explore for 10 min; the behaviour was recorded using EthoVision XT software. The variables observed were (a) the first latency to enter the central zone of the open field arena, (b) the amount of time spent in the central zone, (c) total distance travelled, and (d) mean velocity during the experimental trial.

2.22 | Novelty-induced suppression of feeding

The behavioural assessment was carried out as previously described (Caldji, Francis, Sharma, Plotsky, & Meaney, 2000) with slight modifications. The SD rats were fasted (water was available ad libitum) for 18 hr before the starting day of the experiment. Animals were acclimatized for 1 hr in a dimly lit experiment room on the day of experiment. The behavioural test was carried out in a modified open field set up (diameter 120 cm and height 50 cm) with a dark floor and white coloured walls. A dish filled with standard lab chow was placed in the centre of the field. In the acquisition software (EthoVision XT), the observation area was virtually divided into zones, namely, a feed area, centre, and periphery. Rats were intranasally administered vehicle, relaxin-3 (H3 relaxin), or 14s21 peptide and placed in the periphery of the arena; behaviour was monitored for 10 min. The latency to enter the feed area and the duration of time spent in the feed area and periphery were measured with the EthoVision behaviour tracking and analysis software. The quantity of food consumed and the number of faecal pellets left after each trial were also noted during the trial.

2.23 | Acute and chronic FST

The repeated rat FST was conducted using ForcedSwimScan (CleverSys Inc, Reston, VA, USA). The test involved placing individual rats into a cylindrical tank (transparent acrylic, 45.7 cm height × 20.3 cm width) containing clean water at 25°C on four different occasions (pre-test, test, retest 1, and retest 2). These test conditions have been described previously (Mezadri, Batista, Portes, Marino-Neto, & Lino-de-Oliveira, 2011). On the first day (pretest), the rats were submitted to a 15-min FST (training/pretest), followed by a 5-min trial on Day 2 (test), Day 7 (retest 1), and Day 14 (retest 2). After each session, the rats were taken out of the water and allowed to dry with paper towels for 20–30 min before being returned to their home cages. All the test sessions were videotaped using a camera (WV-CP500, Panasonic, China) positioned at the front of the apparatus to enable subsequent evaluation of the animal behaviour. A rat was observed and tracked within a virtually delineated frame called an “arena.” The arena started just below the surface of the water and was divided into bottom and top zones. Animals received a daily intranasal administration of vehicle, H3 relaxin (275 µg·kg⁻¹), or 14s21 peptide (1.5 mg·kg⁻¹), until Day 14. The experimental schedule is presented in Figure 6a. A rule of thumb for multivariate analyses indicates that at least three cases are required for every variable added to the analysis (Lino-de-Oliveira, De Lima, & de Padua Carobrez, 2005). Immobility was defined as a lack of motion of the whole body consisting only of the small movements necessary to keep the animal's head above the water. Swimming was recorded when large forepaw movements displaced the body around the cylinder, more than necessary to merely keep the head above the water. Climbing was registered when vigorous movements with forepaws in and out of the water, usually directed against the wall of the tank, were observed. Diving was observed when the whole body of the animal, including the head, was submerged

(Mezadri et al., 2011). The behavioural distribution and behavioural categories were considered distinct and separated in time.

2.24 | Randomization and blinding

All culture plate wells for the in vitro experiments and rats for the in vivo experiments were randomized to receive treatments. In vitro and in vivo experiments and data analyses were not performed under blinded conditions because the data acquisition and analyses were standardized and automated with automatic routines built into the analysis programmes. This standardized and automated approach reduced possible operator bias and the need for blinding.

2.25 | Data collection and statistical analysis

The data and statistical analysis comply with the recommendations of the British Journal of Pharmacology on experimental design and analysis in pharmacology (Curtis et al., 2018). For both the in vitro and in vivo experiments, the group sizes for each experiment are provided within the respective methods sections and figure legends. For all the in vivo experiments, the exact number of animals is also provided in Table S2. In vitro assays were performed in $n = 3$ independent repeats of triplicates, unless otherwise stated. When experiments are novel, it is difficult to perform a priori sample size calculations (Curtis et al., 2018) because the effect size and variance are unknown. Therefore, for the animal experiments, estimates of the expected variance and effect size from previous experiments using similar methods were used to estimate appropriate sample sizes a priori through statistical power calculations. The data were recorded (a) by manual food and water intake measurement after every 1 hr and (b) by the LABORAS software, and data obtained over 4 hr were processed and extracted in 10-min-sized bins and exported and tabulated in Excel. Thereafter, statistical analysis was carried out using GraphPad Prism 7 software. Statistical significance was routinely calculated for the behaviour of (relaxin-3 + saline)/(14s21 stapled peptide + saline)/(relaxin-3 + 14s21 stapled peptide) grouped animals in LABORAS cages. The behavioural data from LABORAS home-cage monitoring at various time points were subjected to two-way ANOVA with repeated measures followed by Tukey's post hoc analysis. Bar graphs presenting the mean of values over 80 min were analysed using one-way ANOVA followed by Tukey's post hoc test. For the behavioural experiments, data recorded by the EthoVision software were exported and tabulated in Excel. Thereafter, statistical analysis of these data was carried out using GraphPad Prism software. Statistical analyses of data were performed using one-way ANOVA followed by Tukey's post hoc multiple comparison analysis to determine statistical significance. All statistical analyses conducted were between subjects. Data were tested for normality with a Shapiro–Wilk test. Only normally distributed data were analysed via ANOVA. Additionally, to validate the assumption of equality of variances between groups, Brown–Forsythe and Barlett's tests were conducted in conjunction with the ANOVA. A post hoc Tukey's test was applied only when the F value achieved significance

and there was no significant inhomogeneity of variance. $P < .05$ was considered significant. All the comparisons were made with the vehicle treatment. The results are expressed as the mean \pm SEM. In accordance with Journal requirements, all P values are expressed rounded down to the same threshold value of $P < .05$, and the F statistics are not shown in the main text but are provided in Table S2.

2.26 | Nomenclature of targets and ligands

Key protein targets and ligands in this article are hyperlinked to corresponding entries in <http://www.guidetopharmacology.org>, the common portal for data from the IUPHAR/BPS Guide to PHARMACOLOGY (Harding et al., 2018), and are permanently archived in the Concise Guide to PHARMACOLOGY 2017/18 (Alexander, Christopoulos, et al., 2017; Alexander, Fabbro et al., 2017; Alexander, Kelly et al., 2017).

3 | RESULTS

3.1 | Design, synthesis, and structural analysis of stapled peptides

We first chose to compare the utility of our previously published $i,i+4$ stapled 14s18 peptide (Jayakody et al., 2016) to other stapling chemistries. Conformational analysis revealed that insertion of a 14s18 hydrocarbon linker enhanced α -helicity, whereas the CD spectra of the corresponding 14s18-lactam and 14s18-disulfide bridged peptides indicated that they were random coils (Figures 1a-i,b-i and S1). In an effort to study the minimal effective analogue of the 14s18 peptide, we truncated the 14s18 peptide N-terminus (14s18) and also the control H3 B-chain (H3 B-chain) by removing seven residues. These seven residues were reported not to participate in binding and activation of RXFP3 receptors (Bathgate et al., 2013). Conformational analysis of the 14s18 peptide revealed that the α -helicity was preserved but the overall α -helical content was reduced compared with the full-length 14s18 peptide (Figure 1b-i), highlighting the importance of N-terminus residues that might have some influence in achieving the optimal α -helicity. We and others previously reported that alternative $i,i+4$ stapling positions within the H3 B-chain, for example, at the 18s22 position, were not able to achieve the optimal α -helicity, emphasizing the important consideration of both peptide sequence and the stapling methodology for optimal outcomes (Hojo et al., 2016; Jayakody et al., 2016). Considering the reported structure-activity relationship studies of relaxin-3 (Bathgate et al., 2013; Wong et al., 2018) and molecular modelling of various staple combination scans over the entire H3 B-chain sequence, we identified the optimal positions for $i,i+7$ staples at 14s21 and 11s18 positions (Figures 1a-ii and S1). Additionally, to understand the effect of Cys10/22 to Ser substitutions in the H3 B-chain, we opted to keep the $i,i+7$ peptides (14s21 and 11s18) in the natural sequence of the H3 B-chain, that is, without mutating the Cys 10/22 to Ser, and compare them with a control peptide in which Cys10/22 were mutated to Ser (14s21-Ser).

Both the Cys-containing $i,i+7$ stapled peptides 14s21 and 11s18 were successfully synthesized and exhibited up to 23.5-fold and 21.9-fold α -helix stabilization respectively (Figure 1b-ii). In fact, it was reported that the $i,i+7$ hydrocarbon staple can serve as a powerful nucleator of the α -helical structure, such that incorporation of a single staple in a short stretch of a peptide can promote helicity throughout a much longer sequence (Bird et al., 2010; Walensky & Bird, 2014). All the peptides listed in Table 1 were readily synthesized and were used for bioassays (Table S1).

3.2 | In vitro activity and stability of stapled peptides

Saturation binding studies conducted with Eu-DTPA-R3 B1-22R in HEK-RXFP3 cells showed a single population of sites with a density of $1,061 \pm 46.68$ fmol \cdot mg $^{-1}$ with apparent binding affinity of 35 nM (Jayakody et al., 2016). Competitive binding with the test stapled peptides revealed that the 14s18 peptide showed improved binding affinity compared with the H3 B-chain (Figure 2a-i and Table 2; Jayakody et al., 2016). We also utilized a previously reported, highly potent, minimized H3 B-chain analogue, which is an N-terminus seven-residue truncated 13s17 stapled peptide (13s17; Hojo et al., 2016), as a control test peptide to compare the binding affinity of the 14s18 peptide. The 13s17 peptide exhibited an improved binding affinity of 151 nM, as reported previously, and the 14s18 peptide was not able to produce a similar effect on receptor binding (Figure 2a-ii and Table 2). 14s18 was also able to stimulate cAMP activation with an EC₅₀ of 43 nM, but this stimulation was weaker than that of the full-length 14s18 peptide (17 nM; Figure 2b-i and Table 2). The 14s18-lactam and 14s18-disulfide demonstrated very weak binding affinity and potency for RXFP3 receptors (Figure 2a-ii,b-ii and Table 2). Of the $i,i+7$ staples (14s21 and 11s18), 14s21 retained the most potent competitive binding, with clear increase over the H3 B-chain (pKi = 66 nM) and a clear increase in cAMP activity (pEC₅₀ = 3 nM; Figure 2a-iii,b-iii and Table 2). The Cys to Ser substitution in the 14s21 peptide (14s21-Ser) did not have major effect on the binding affinity, but 14s21-Ser was not as potent as the Cys-containing 14s21 peptide (Figure 2a-iii, b-iii and Table 2). The 11s18 peptide displayed a moderate binding affinity of 331 nM and cAMP inhibitory activity with an EC₅₀ value of 17 nM (Figure 2a-iii,b-iii and Table 2). This suggests that the edge of the N-terminus helix may not provide a significant interaction with RXFP3 receptor. In an ERK1/2 kinase phosphorylation assay, the 14s21 peptide displayed dose-dependent activity, similar to H3 relaxin [H3 relaxin, pEC₅₀ = 10.04 ± 0.12 ($n = 3$) and the 14s21 peptide, pEC₅₀ = 9.74 ± 0.09 ($n = 3$); Figure 2c]. To examine the effect of stapling on conformational stability, a variable temperature-CD assay was performed and showed that both the $i,i+4$ and $i,i+7$ stapled peptide underwent a cooperative melting transition (T_m range of 50–55°C; Figure 2d), indicating high conformational stability. To measure the comparative protease susceptibility, we subjected the peptides to trypsin digestion over a time period of 25 hr. $i,i+4$ stapling conferred up to a 1.6-fold enhancement in peptide $t_{1/2}$ compared with the unmodified peptide, whereas the $i,i+7$ stapled analogue manifested

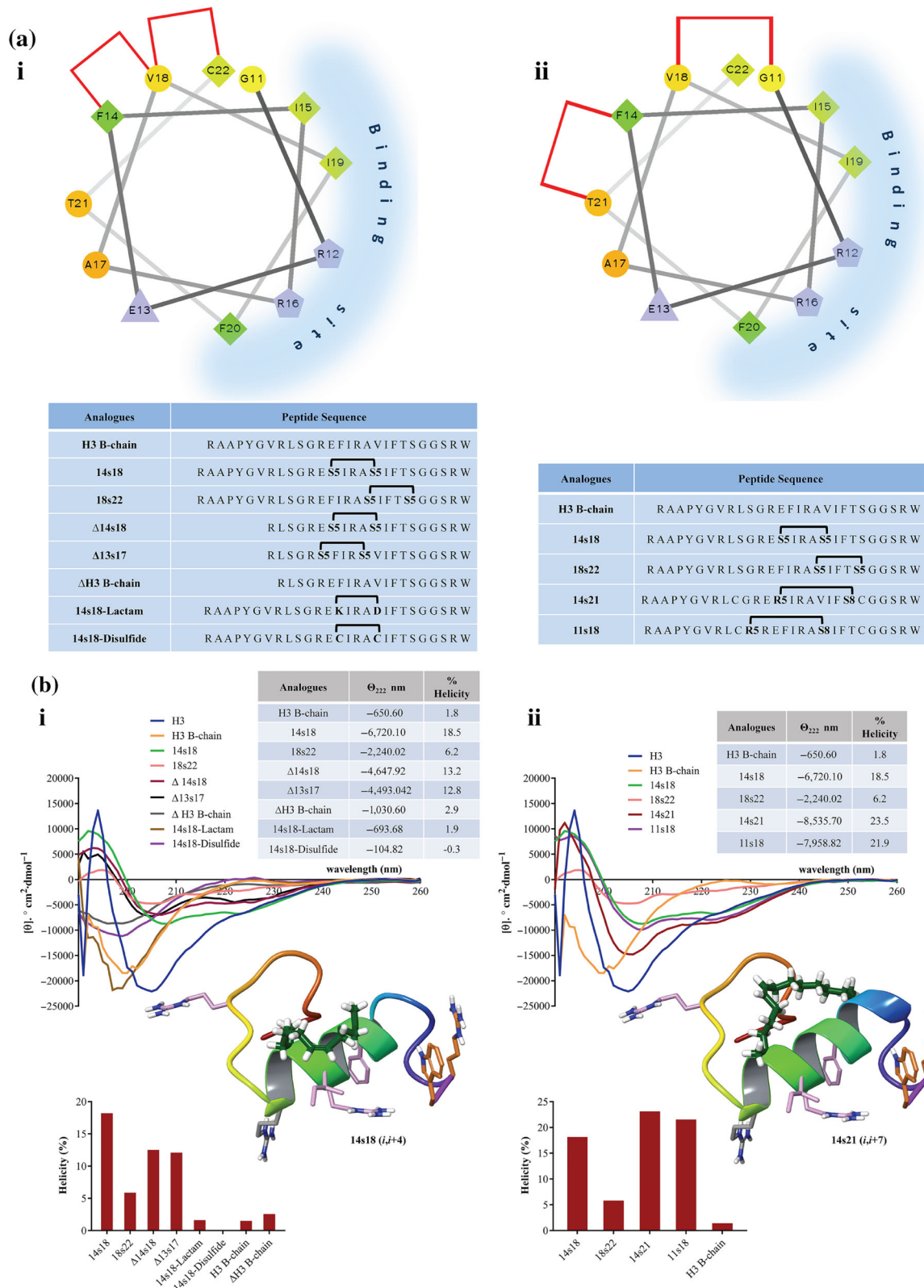


FIGURE 1 Design, sequence composition, and structural analysis of stapled peptides. (a) Helix wheel projections of (i) $i,i+4$ stapled peptides (14s18 and 18s22) and (ii) $i,i+7$ stapled peptides (14s21 and 11s18). Different positions of the staples correspond to the analogues shown in the corresponding tables. (b) Circular dichroism analysis of stapled peptides and variants, demonstrating the observed range of α -helical stabilization induced by hydrocarbon stapling. (i) $i,i+4$ and (ii) $i,i+7$ hydrocarbon staples manifest substantial structural stabilization compared with the unstapled H3 B-chain and the lactam and disulfide variants of the 14s18 hydrocarbon staple. One $i,i+4$ staple (14s18) and both $i,i+7$ staples (14s21 and 11s18) of the H3 B-chain sequence yielded peptides with marked α -helicities. The bar diagram shows the per cent helicity of all the peptides compared with that of the H3 B-chain. The ribbon diagram shows the reinforced α -helical structure of the 14s18 ($i,i+4$) and 14s21 ($i,i+7$) peptide ligands

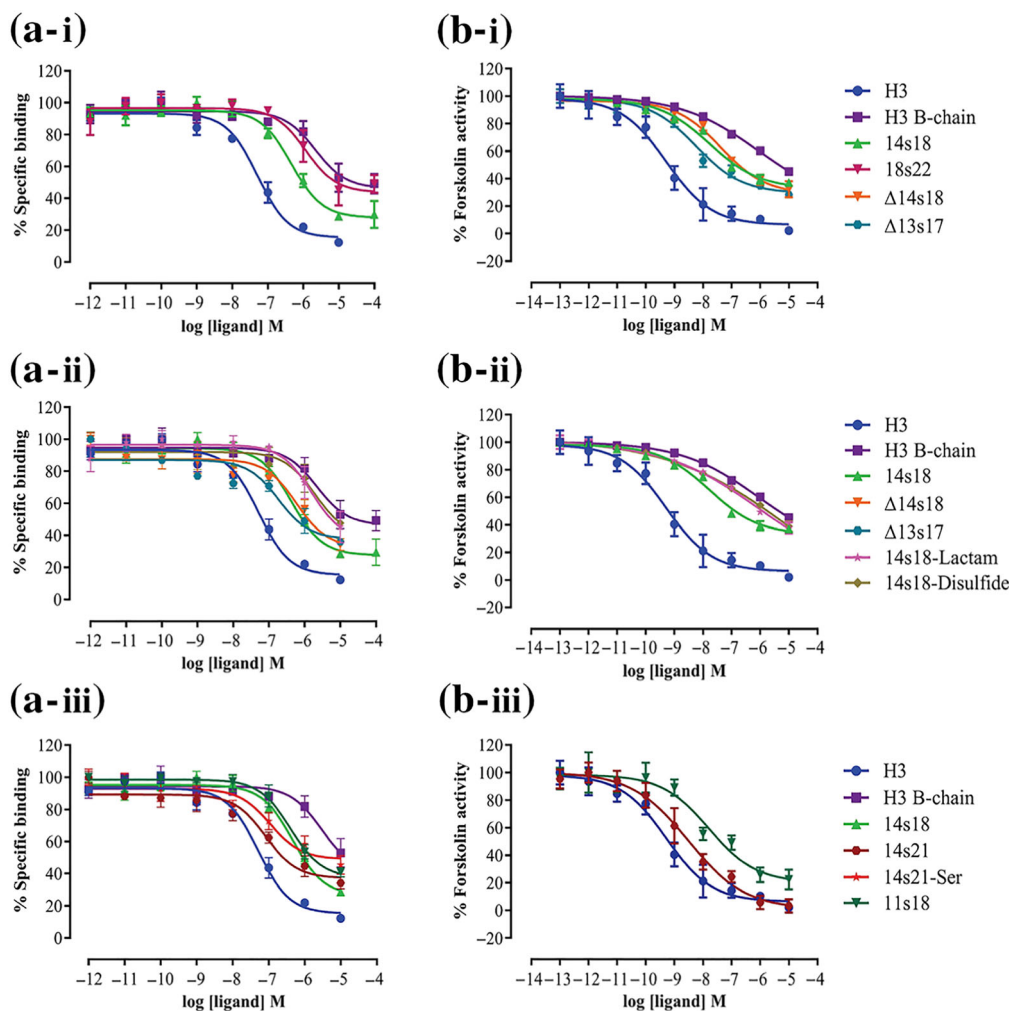


FIGURE 2 In vitro activity and stability profiles of H3 B-chain stapled peptide analogues. (a) Competition binding curves for H3 B-chain stapled peptide analogues in HEK-RXFP3 cells using Eu-DTPA-R3B1-22R as the labelled ligand. Various concentrations of (i) H3 (1 pM–10 μM H3) and stapled peptides (1 pM to 100 μM for 14s18, 18s22, and the H3 B-chain); (ii) the full-length 14s18 stapled peptide and 14s18 staple variants (14s18-lactam and 14s18-disulfide peptides; 1 pM to 100 μM) and N-terminus truncated Δ14s18 and Δ13s17 peptides (1 pM to 10 μM); and (iii) the $i,i+7$ stapled peptides 14s21, 14s21-Ser, and 11s18 compared with the ($i,i+4$) 14s18 peptide (1 pM to 10 μM) were tested. The data are presented as the mean ± SEM of triplicate samples from three to four independent experiments. (b) Inhibition of forskolin-induced cAMP activation in HEK-RXFP3 cells by (i) H3, the H3 B-chain, 14s18, and the N-terminus truncated Δ14s18 and Δ13s17 peptides (0.1 pM to 10 μM). (ii) cAMP activation profiles of the full-length 14s18 stapled peptide and 14s18 staple variants (14s18-lactam and 14s18-disulfide peptides; 0.1 pM to 10 μM) and (iii) the $i,i+7$ stapled peptides (14s21, 14s21-Ser, and 11s18), H3, and the H3 B-chain (0.1 pM to 10 μM). The cAMP concentration is presented as a percentage of the forskolin-induced response (mean ± SEM; $n = 3$). (c) Western blot showing that H3 and 14s21 induce dose-dependent increases in ERK1/2 phosphorylation. Representative dose–response curves for the effect of H3 and 14s21 peptide on ERK1/2 kinase phosphorylation in HEK-RXFP3 cells. The data are presented as the mean ± SEM of triplicate samples from three independent experiment. (d) Thermodynamic stability of stapled peptides. Temperature-dependent thermal unfolding curves for the $i,i+7$ stapled peptides 11s18 and 14s21 and an $i,i+4$ stapled peptide, depicting the linear dependency and partially unfolded nature of the peptides upon heating. (e) Proteolytic stability of stapled peptides. Trypsin resistance profiles of the H3 B-chain and the 14s18 ($i,i+4$) and 14s21 ($i,i+7$) stapled peptides over a time period of 25 hr. The data (mean ± SEM) represent the per cent fraction intact in experiments

4.5-fold enhancement (Figure 2e). From a mechanistic standpoint, the longer $i,i+7$ staple not only slowed the kinetics of proteolytic digestion but completely eliminated cleavage of two arginine sites that were either localized within the protective umbrella of the staple or were immediately adjacent to it (Figure S2). Taken together, these data demonstrate that the $i,i+7$ stapled 14s21 peptide exhibits optimized α -helicity and protease resistance and is a structurally stable, high-affinity, and potent agonist ligand of RXFP3 receptors.

3.3 | Effect of central administration of H3 relaxin and 14s21 peptide on food and water intake and related behaviour in rats

Relaxin-3 (H3) is known to be an orexigenic peptide that produces dose-dependent effects in rats (Calvez et al., 2017; McGowan et al., 2006; Otsubo et al., 2010). A single high-dose intracerebroventricular injection of H3 relaxin to satiated male SD rats significantly increased

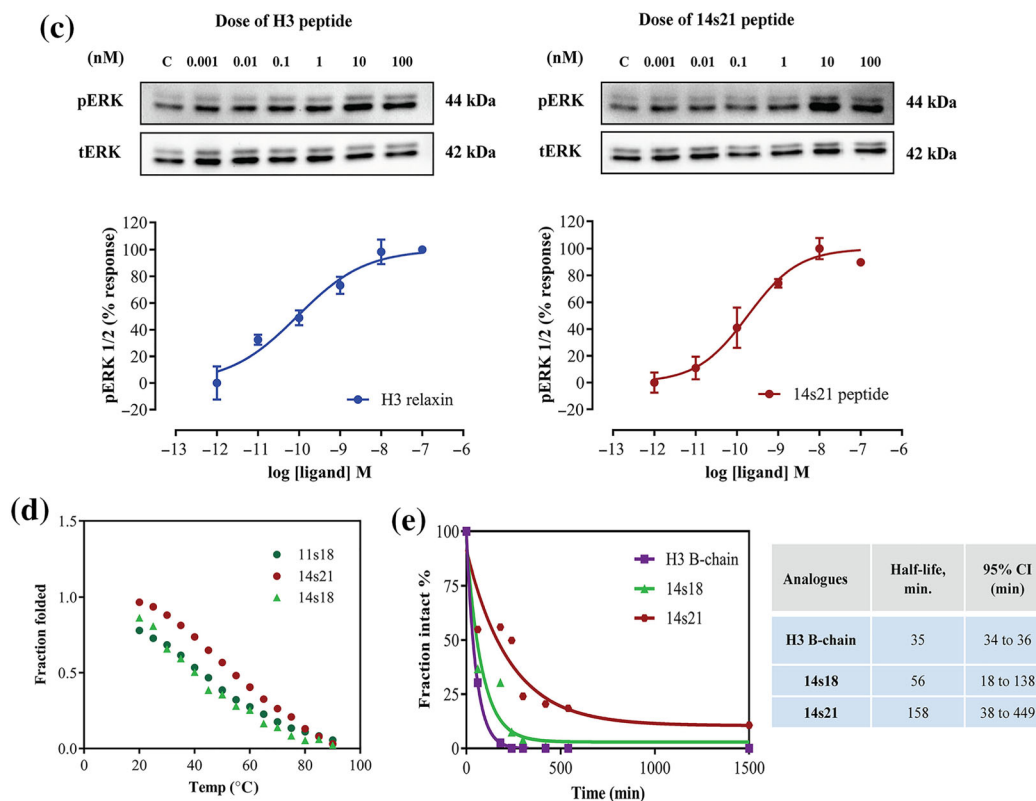


FIGURE 2 Continued.

food intake in the first hour post-administration (Figure S3). The optimal pEC_{50} value reported for the 14s21 stapled peptide (8.51 ± 0.07) in our lab was approximately 10-fold less than the H3 relaxin pEC_{50} value (9.28 ± 0.15), and thus, we used an equivalent dose of H3 relaxin (0.1 nmol) to compare the equivalent activity reported by the 14s21 peptide (1 nmol). Single intracerebroventricular administration of 14s21 peptide to satiated rats in the early light phase significantly increased food intake within the first hour after injection (Figure 3b; 0- to 1-hr food intake: 0.84 ± 0.07 g [vehicle], 3.74 ± 0.1 g [H3 relaxin: 0.1 nmol]; 3.41 ± 0.15 g [14s21 peptide: 1 nmol]; $n = 6$ rats per group). Cumulative food and water intake were significantly increased at 2, 3, and 4 hr post-intracerebroventricular administration of H3 relaxin and 14s21 peptide (Figure 3c-i,c-ii). A detailed analysis for up to 4 hr in a LABORAS home-cage environment revealed significant difference between the effects of H3 relaxin and 14s21 peptide treatment on different behaviour paradigms (Figure 3d-i,d-vi; Table S2).

3.4 | Evaluation and optimization of intranasal drug delivery of H3 relaxin and 14s21 peptide in rats

In our current approach, we first optimized the experimental factors in rats, such as head position, volume, and method of administration, which can influence drug deposition within the nasal passage and pathways leading into the CNS (Dhuria, Hanson, & Frey, 2009; Lukas & Neumann, 2012). In preliminary experiments, several different H3 relaxin concentrations (2.75 , 27.5 , 275 , and $2,750 \mu\text{g}\cdot\text{kg}^{-1}$) were intranasally administered. Dose-response studies revealed that H3

relaxin treatment had a significant effect (eating behaviour and drinking behaviour: one-way ANOVA, Figure 4b-i). Post hoc Tukey's test revealed that $275 \mu\text{g}\cdot\text{kg}^{-1}$ and $2,750 \mu\text{g}\cdot\text{kg}^{-1}$ doses were significantly effective in stimulating both eating and drinking behaviour. Therefore, we first chose the optimal $275 \mu\text{g}\cdot\text{kg}^{-1}$ dose of H3 relaxin to analyse its effect on related behaviour paradigms. H3 relaxin ($275 \mu\text{g}\cdot\text{kg}^{-1}$) was delivered intranasally to rats, and their behaviour in LABORAS was analysed. After optimization of behaviour parameters with H3 relaxin, we undertook similar dose-response relationship studies for the 14s21 peptide (0.015, 0.15, 1.5, and $15 \text{ mg}\cdot\text{kg}^{-1}$) and found that the treatment had a significant effect (Figure 4b-ii). A post hoc Tukey's test revealed a significant increase in eating behaviour with $0.15 \text{ mg}\cdot\text{kg}^{-1}$, $1.5 \text{ mg}\cdot\text{kg}^{-1}$ and $15 \text{ mg}\cdot\text{kg}^{-1}$ 14s21 peptide. However, the 14s21 peptide was able to elicit the drinking behaviour only at a $1.5 \text{ mg}\cdot\text{kg}^{-1}$ concentration (Figure 4b-ii). After successful dose optimization, we performed a detailed analysis of behaviour for up to 4 hr in a LABORAS home-cage environment after administration of $275 \mu\text{g}\cdot\text{kg}^{-1}$ H3 relaxin and $1.5 \text{ mg}\cdot\text{kg}^{-1}$ 14s21 peptide (Figure 4c-i,c-vi). Interestingly, the effect of the 14s21 peptide lasted longer than that of H3 relaxin based on analysis in the LABORAS behaviour paradigm. Previous studies have also demonstrated sex-specific effects on increased food intake in female rats compared with male rats when given a higher dose of intracerebroventricular H3 relaxin (Calvez et al., 2017; Calvez, Lenglos, de Avila, Guevremont, & Timofeeva, 2015). However, no sex-specific differences were observed in eating and drinking behaviour after intranasal H3 relaxin ($275 \mu\text{g}\cdot\text{kg}^{-1}$) and 14s21 peptide

TABLE 2 Competitive binding activity (pK_i) and functional in vitro cAMP activity (pEC_{50}) values for H3 B-chain analogues

| Analogue | Eu-DTPA-R3(B1-22R) pK_i | cAMP pEC_{50} |
|-----------------|---------------------------|---------------------------|
| H3 relaxin | 7.38 ± 0.11 [41.69 nM] | 9.28 ± 0.15 [0.52 nM] |
| H3 B-chain | 5.75 ± 0.24 [1,778.28 nM] | 6.02 ± 0.24 [955.10 nM] |
| 14s18 | 6.42 ± 0.13 [380.19 nM] | 7.77 ± 0.13 [16.98 nM] |
| 18s22 | 6.02 ± 0.23 [955.10 nM] | n.d. |
| 14s18 | 6.32 ± 0.24 [478.63 nM] | 7.37 ± 0.14 [42.65 nM] |
| 13s17 | 6.82 ± 0.25 [151.36 nM] | 8.24 ± 0.15 [5.75 nM] |
| 14s18-Lactam | 5.89 ± 0.27 [1288.25 nM] | 5.97 ± 0.71 [1,071.52 nM] |
| 14s18-Disulfide | 5.80 ± 0.40 [1,580.90 nM] | 4.78 ± 1.5 [16.5 μ M] |
| 14s21 | 7.18 ± 0.20 [66.07 nM] | 8.51 ± 0.07 [3 nM] |
| 14s21-Ser | 7.05 ± 0.26 [89.12 nM] | 8.28 ± 0.16 [5.24 nM] |
| 11s18 | 6.48 ± 0.14 [331.13 nM] | 7.78 ± 0.14 [16.65 nM] |

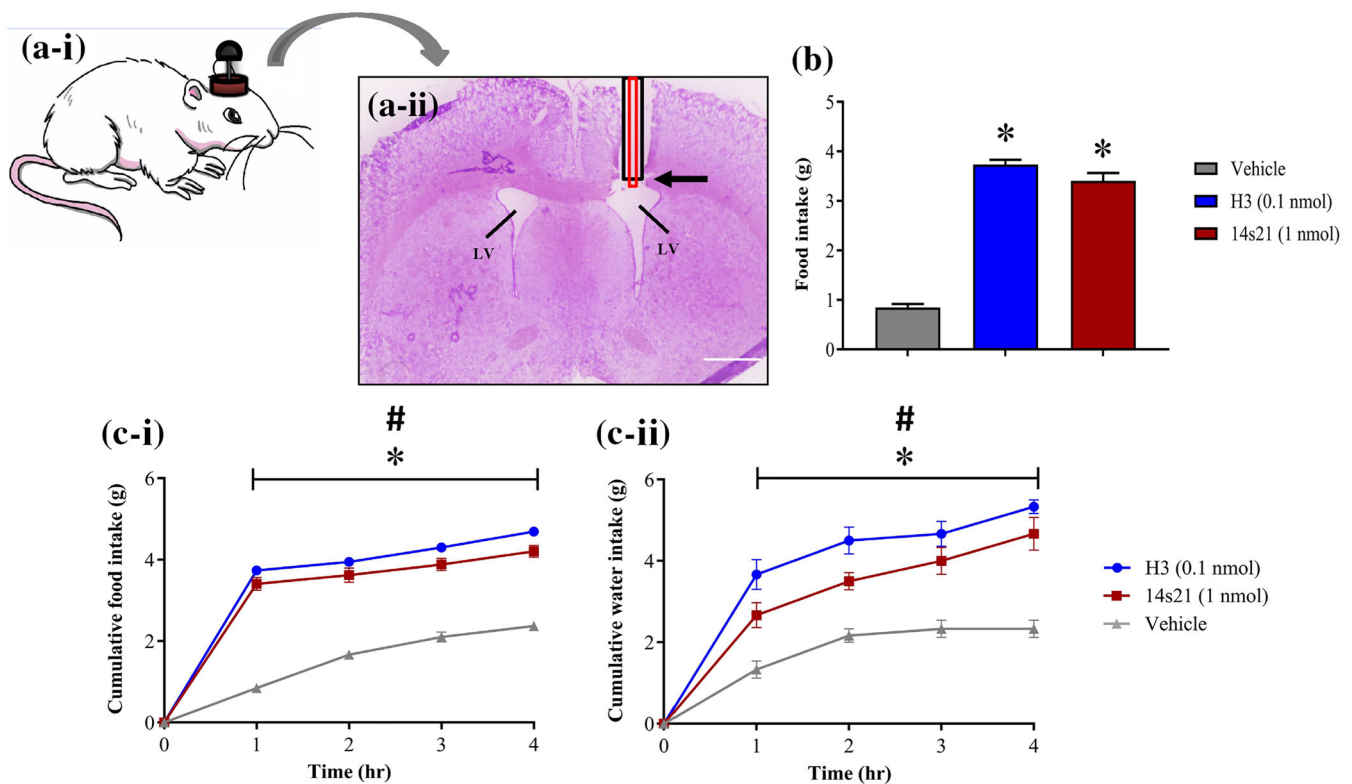


FIGURE 3 In vivo demonstration of the effect of H3 relaxin and 14s21 peptide administration through intracerebroventricular injection on eating, drinking, and locomotory behaviour in male SD rats. (a-i) Pictorial presentation showing a rat with an implanted cannula and (a-ii) representative micrograph of a Nissl-stained brain section showing the track left by the guide cannula (black line) and the injection cannula (red line) position in the lateral ventricle (marked by an arrow) at 1 \times (scale bar represents 1 mm). (b) Effect of intracerebroventricular injection of H3 (0.1 nmol) and 14s21 peptide (1 nmol) on 1-hr food intake in the early light phase in satiated male SD rats. * $P < .05$, significantly different from vehicle. (c) Effect of intracerebroventricular administration of H3 (0.1 nmol) and 14s21 peptide (1 nmol) on (i) cumulative food intake and (ii) cumulative water intake over 4 hr in the early light phase. (d) Two-way ANOVA with 10-min time bins recorded for up to 4 hr in a LABORAS home-cage environment revealed significant differences from vehicle, in time spent in eating behaviour (d-i), time spent in drinking behaviour (d-ii), time spent in grooming (d-iii), time spent in rearing (d-iv), time spent in locomotion (d-v), and total distance travelled (d-vi). Data points represent the mean of the parameter over the preceding 10 min (d-i to d-vi). One-way ANOVA followed by Tukey's post hoc conducted on data collected in the first 80 min indicated that both the peptide treatments had a significant effect on all the above measured parameters. Columns represent the mean (with SEM) of values over 80 min (insets in d-i to d-vi). Shaded areas represent the total activity recorded in the first 80 min after drug administration. $n = 6$ rats per group. * $P < .05$, significantly different from vehicle; one- or two-way ANOVA followed by Tukey post hoc multiple comparison

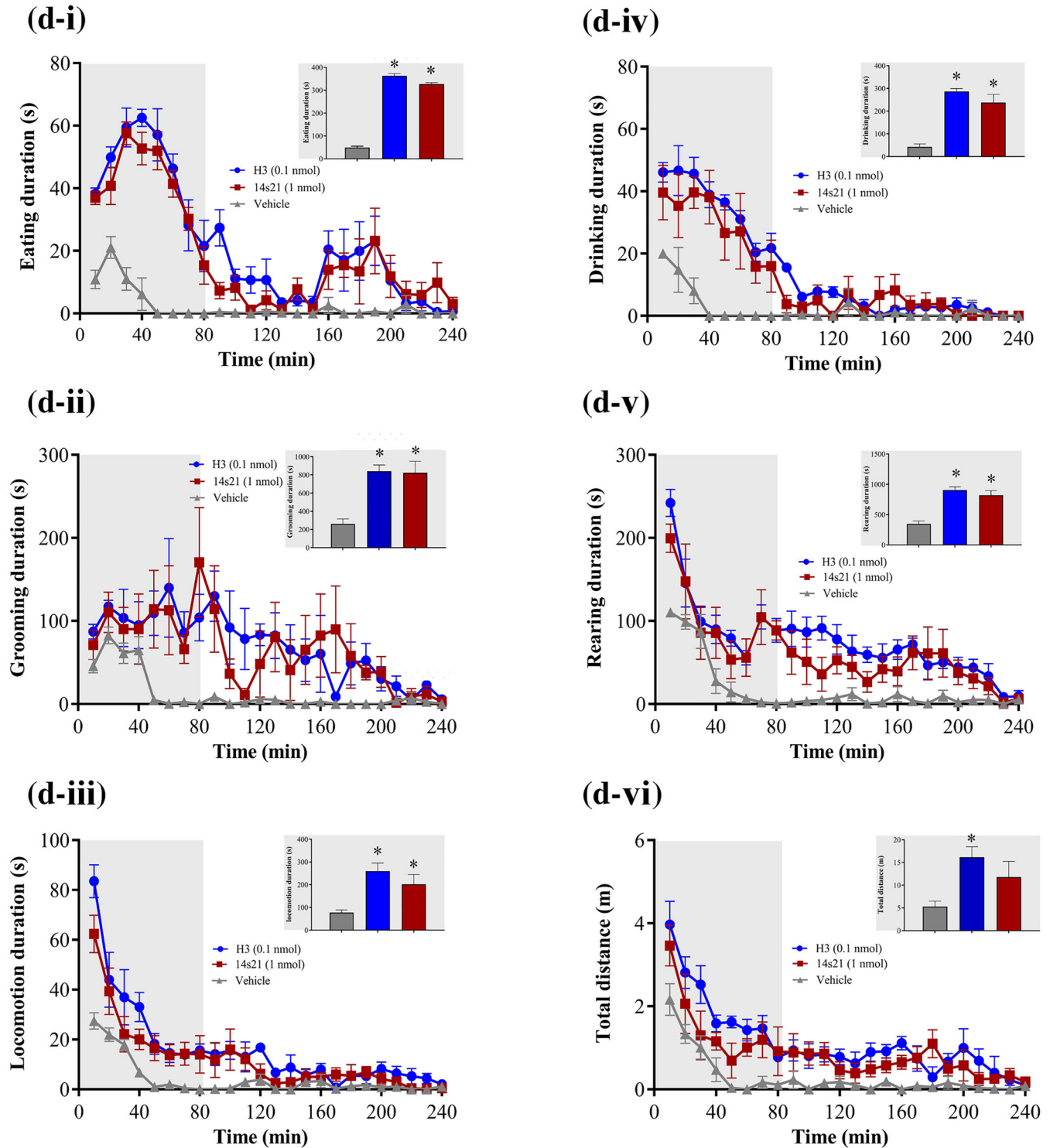


FIGURE 3 Continued.

(1.5 mg·kg⁻¹) treatment (Figure 4d; Table S2). After successful optimization and establishment of intranasal administration of H3 relaxin and 14s21 peptide and with the required evidence pertinent to metabolism/eating disorders, we attempted to optimize the behaviour models that are relevant and potentially translatable to the treatment of major depression and anxiety disorders.

3.5 | Intranasal treatment with H3 relaxin and 14s21 peptide in anxiety-related behaviour paradigms

We chose the optimal response time of H3 relaxin (275 µg·kg⁻¹) and 14s21 peptide (1.5 mg·kg⁻¹) or vehicle when the maximal activity was recorded in LABORAS. Thus, 30 min after H3 relaxin and 14s21

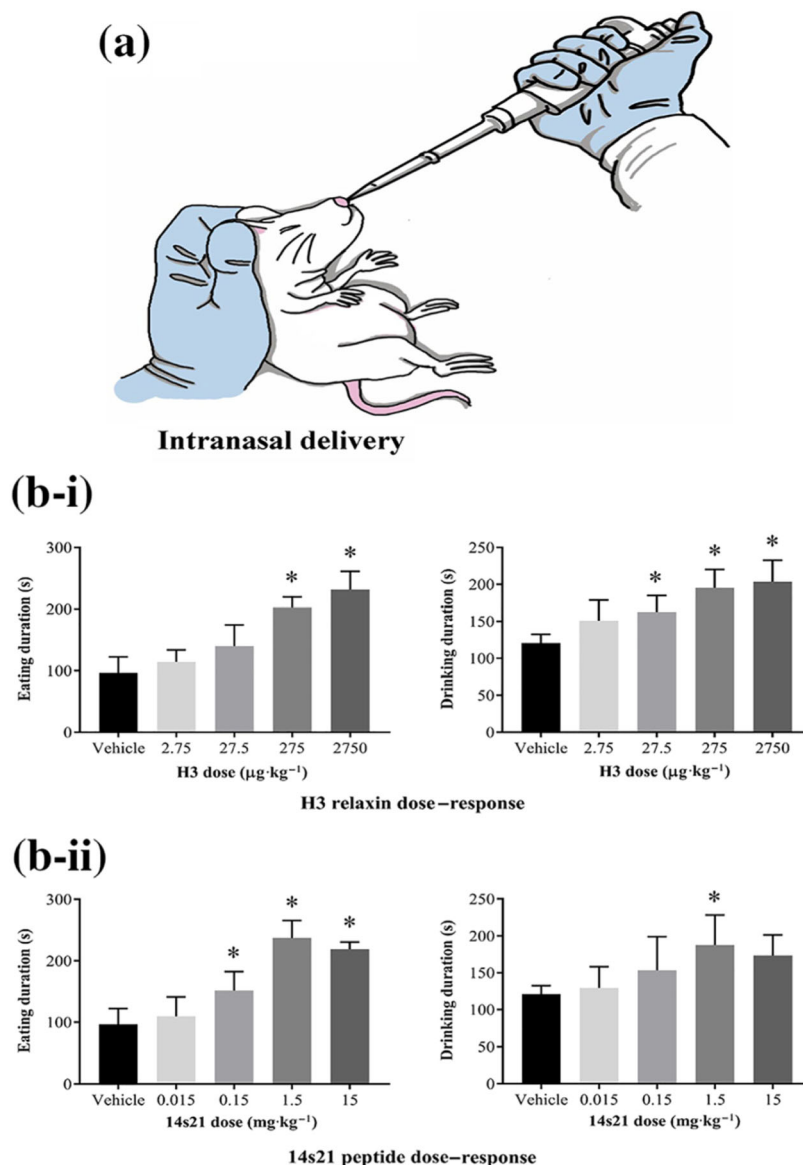


FIGURE 4 Stimulation of eating and drinking behaviour following intranasal administration of different H3 relaxin and 14s21 peptide doses. (a) Pictorial diagram showing rat position during intranasal administration. (b) Concentration-response curves for the intranasal administration effects of H3 and 14s21 peptide. Intranasal administration of H3 (2.75, 27.5, 275, and 2750 $\mu\text{g}\cdot\text{kg}^{-1}$) and 14s21 peptide (0.015, 0.15, 1.5, and 15 $\text{mg}\cdot\text{kg}^{-1}$) was demonstrated to be efficient in activating the receptor at doses equivalent to or higher than those used in intracerebroventricular administration. Changes in eating and drinking behaviour were recorded in LABORAS over 80 min immediately after peptide administration. (b-i) The H3 relaxin-treated groups (275 and 2750 $\mu\text{g}\cdot\text{kg}^{-1}$) displayed a significant increase in food intake and drinking behaviour in comparison with the vehicle-treated group. (b-ii) 14s21 peptide administration at 0.015, 0.15, and 1.5 $\text{mg}\cdot\text{kg}^{-1}$ concentrations led to a significant increase in food intake, whereas only the 1.5 $\text{mg}\cdot\text{kg}^{-1}$ dose of 14s21 peptide elicited drinking behaviour. (c) Effect of intranasal administration of H3 (275 $\mu\text{g}\cdot\text{kg}^{-1}$) and 14s21 peptide (1.5 $\text{mg}\cdot\text{kg}^{-1}$) in satiated SD rats analysed over 4 hr (240 min) via LABORAS home-cage activity monitoring. Data points represent the mean of the parameters over the preceding 10 min (c-i to c-vi). Two-way ANOVA in the data across time showed significant changes in eating behaviour (c-i), drinking behaviour (c-ii), rearing duration (c-iii), and locomotion (c-iv). There was an overall significant difference in grooming behaviour (c-v) and total distance travelled (c-vi) across the entire 4-hr paradigm. The columns represent mean (with SEM) of values over 80 min (insets in c-i to c-vi). The data across the first 80 min showed significant differences between the treatments (H3 relaxin and 14s21 peptide) and vehicle for the time spent in eating, drinking, rearing, and total distance travelled; one-way ANOVA. Other parameters, time spent in grooming and time spent in locomotion, were not significantly affected by treatment with either of the peptides (insets in c-i to c-vi). (d) Comparison of (i) eating and (ii) drinking behaviour in male and female SD rats ($n = 6$ rats per group) analysed over 2 hr in LABORAS immediately after intranasal administration of H3 (275 $\mu\text{g}\cdot\text{kg}^{-1}$) and 14s21 peptide (1.5 $\text{mg}\cdot\text{kg}^{-1}$). No sex-specific differences were observed, and the difference between sexes was not significant. The data represent the mean \pm SEM $n = 6$ rats per group. * $P < .05$, significantly different from vehicle groups with the same sex and under the same treatment conditions; one-way or two-way ANOVA followed by Tukey's multiple comparison analysis

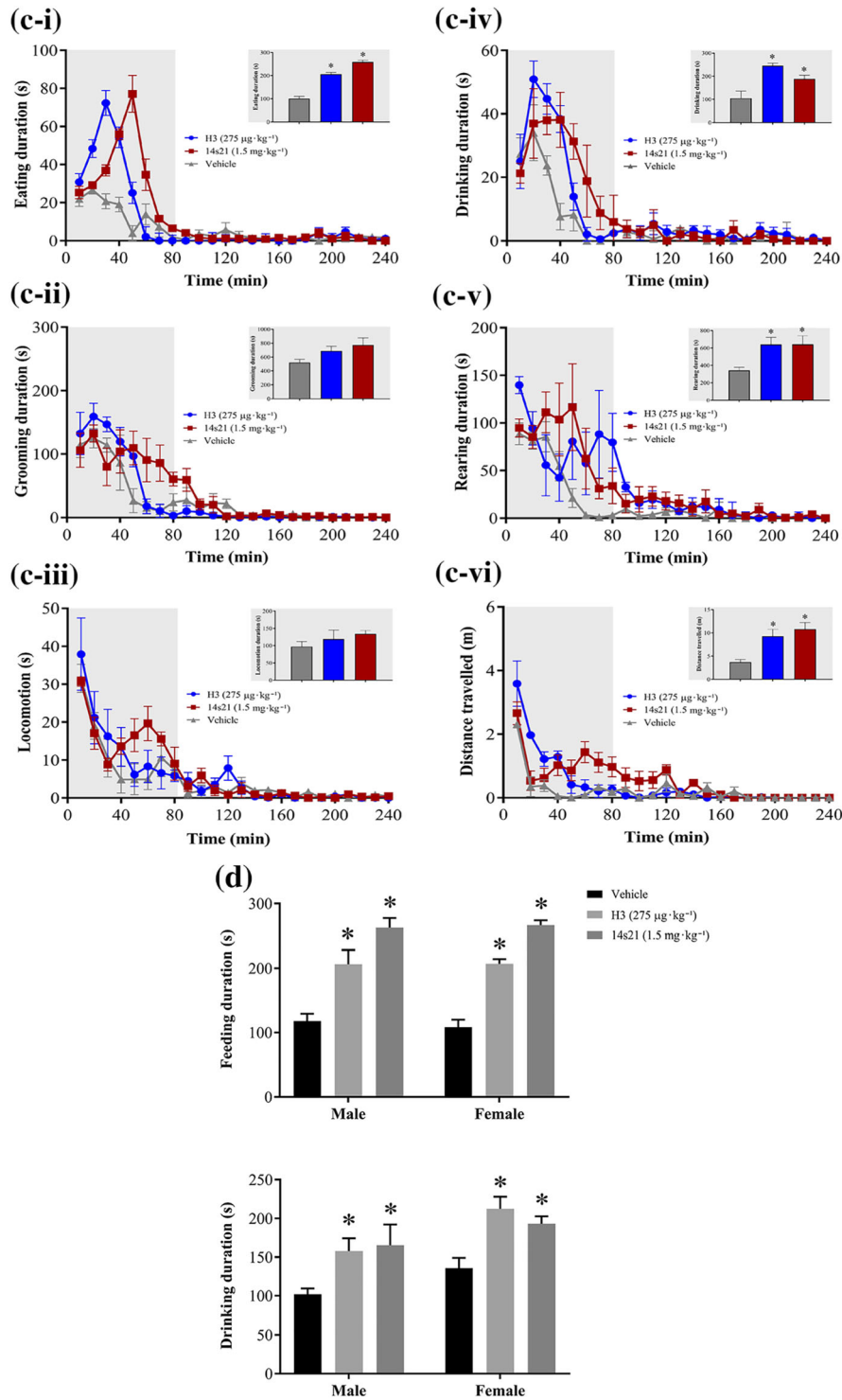


FIGURE 4 Continued.

peptide intranasal administration, the behaviour of rats in an EZM, LDB, open field test, and NSFT was recorded. The effect of intranasal H3 relaxin and 14s21 peptide was found to be significant in all the parameters analysed in the EZM (Figure 5a-i,a-iv). In the LDB test, H3 relaxin and 14s21 peptide displayed significant effects on the time spent in the light zone and number of entries made into the light zone (Figure 5b-i,b-ii). Using automated tracking of the rat centroid, we also

computed the distance travelled in the light and dark areas of the LDB (Figure 5b-iii). H3 relaxin and 14s21 peptide also showed significant differences in the activity parameters assessed in the open field test (Figure 5c). In the NSFT, both H3 relaxin and 14s21 peptide significantly altered the time spent in the centre and latency to reach the food (Figure 5d-i,d-ii), but only 14s21 peptide treatment led to a significant increase in velocity (Figure 5d-iii), and no significant

differences in total distance travelled was observed after either of the peptide treatments (Figure 5d-iv). Corresponding heat maps represent the cumulative time spent in the experimental arena after treatment with vehicle, H3 relaxin, or 14s21 peptide treatment (Figure 5). Thus, both H3 relaxin and 14s21 peptide showed a significant anxiolytic effect in the behaviour paradigms. However, the effect of the 14s21 peptide was slightly better than that of H3 relaxin in the above behavioural paradigms.

3.6 | Antidepressant activity of H3 relaxin and 14s21 peptide in a repeat rat FST

We used a modified protocol of the repeat rat FST within the subject design (Mezadri et al., 2011). SD rats were submitted to 15 min of training (Day 1: pretest) followed by three subsequent 5-min swimming tests 1 week apart (Day 2: test, Day 7: retest 1, and Day 14: retest 2; Figure 6a). To validate the methods, daily intranasal administration of H3 relaxin ($275 \mu\text{g}\cdot\text{kg}^{-1}$) and 14s21 peptide ($1.5 \text{ mg}\cdot\text{kg}^{-1}$) or vehicle was given over a 2-week period. Tests and retests were further scored for the duration of immobility, swimming, and climbing behaviours. On the first day of training, H3 relaxin- and 14s21 peptide-treated animals showed a slight decrease in immobility, but the effect did not reach statistical significance (Figure 6b). After 24 hr of training, the rats were subjected to a 5-min FST procedure [test-acute study]. Both H3 relaxin and 14s21 peptide induced a significant decrease in rat immobility (one-way ANOVA followed by Tukey's HSD, H3 relaxin; $P < .05$ vs. vehicle, 14s21 peptide; $P < .05$ vs. vehicle; Figure 6c-i). H3 relaxin and 14s21 both induced a significant increase in the climbing behaviour (Figure 6c-ii). In retest 1 [retest 1-subacute study], the duration of immobility was further significantly decreased by H3 relaxin and 14s21 peptide (Figure 6d-i). Climbing behaviour was also found to be significantly increased (Figure 6d-ii). In retest 2, the effect of chronically administered 14s21 peptide was significant in reducing the immobility duration of the animals (Figure 6e-i). When chronically administered, both H3 relaxin and 14s21 peptide increased the climbing behaviour significantly (Figure 6e-ii). No significant difference was observed in swimming behaviour elicited by H3 relaxin or 14s21 peptide in the entire repeat FST paradigms (Figure 6; Table S2).

4 | DISCUSSION

We demonstrated here that an $i,i+7$ stapled 14s21 peptide efficaciously maintained the α -helical conformation of the H3 B-chain sequence, leading to high-affinity binding and an approximately 300-fold increase in potency in activating RXFP3 receptors. The extent of α -helix stabilization by both $i,i+4$ and $i,i+7$ staples may vary from peptide to peptide and from position to position within a given peptide sequence (Cromm, Spiegel, & Grossmann, 2015; Walensky & Bird, 2014). Bioinformatic modelling approaches to stapled peptide design have demonstrated that the identification of quasi-stable "dummy" states in the unfolded peptide diminishes helix stability (Guo et al.,

2010). As these events are not trivial to predict, synthesis and thorough empirical in vitro analysis of panels of staple-permuted peptides materializes as the most efficacious route to identify a lead compound having optimal receptor affinity, efficacy, and stability (Chapuis et al., 2012; Walensky et al., 2004). We further showed that intracerebroventricular administration of the 14s21 peptide significantly increased food intake and exhibited properties similar to those of relaxin-3 in vivo, suggesting agonist activity at rat RXFP3 receptors.

We explored whether intranasal delivery held promise as a route of administration for relaxin-3 peptide drugs. Recent studies with insulin, neuropeptide S, oxytocin, and vasopressin (Hallschmid et al., 2008; Ionescu et al., 2012) suggest that intranasal delivery might enable bypassing of the blood-brain barrier to modulate behaviour. Our findings confirmed that centrally, as well as intranasally administered, relaxin-3 and 14s21 peptide have an orexigenic effect. At present, the mechanisms by which stapled peptides are intranasally transported are poorly understood, as are the structural features of these peptides that are responsible for uptake. In the present study, we combined peptide stapling and intranasal delivery, and to the best of our knowledge, this is the first time these combined technologies have been applied to the relaxin-3/RXFP3 receptor system to enable brain exposure via a non-invasive route. Here, we also reported the best optimized full-length H3 B-chain stapled peptide (14s21) compared with the native relaxin-3 peptide (H3). We used both male and female SD rats in our current study. Male SD rats were tested first in an intracerebroventricular administration experiment followed by intranasal administration studies with male SD rats and female SD rats. It has been reported that differential effects of H3 relaxin on CRH expression in the PVN and BNST may contribute to sex-specific differences in behavioural responses (Calvez et al., 2017). However, we found no statistically significant sex-specific differences in feeding or drinking after intranasal administration.

As required by the National University of Singapore Institutional Animal Care and Use Committee and journal publication requirements (Curtis et al., 2018; McGrath & Lilley, 2015), we have considered the possible implications for the replacement, refinement, or reduction of the use of animals in research. Intranasal administration offers a refinement over intracerebroventricular administration because it is less invasive.

Both H3 relaxin and 14s21 peptide significantly increased the rat food intake within the first 80 min after intranasal drug administration. This transient hyperphagia might be explained by the fact that relaxin-3 analogues activate the MAPK/ERK signalling pathway in septal cholinergic neurons of the MS/DB (Albert-Gasco et al., 2017) and support the putative mechanism by which NI relaxin-3 projections regulate the septo-hippocampal system (Olucha-Bordonau et al., 2012). The 14s21 peptide elicited a dose-dependent increase in ERK1/2 phosphorylation and showed the same potency as H3 relaxin. The potency of H3 relaxin in the current study was consistent with that reported in earlier in vitro studies (van der Westhuizen, Werry, Sexton, & Summers, 2007). Orexigenic actions exerted by intranasal H3 relaxin and the 14s21 peptide are consistent with evidence indicating that acute and chronic central administration of

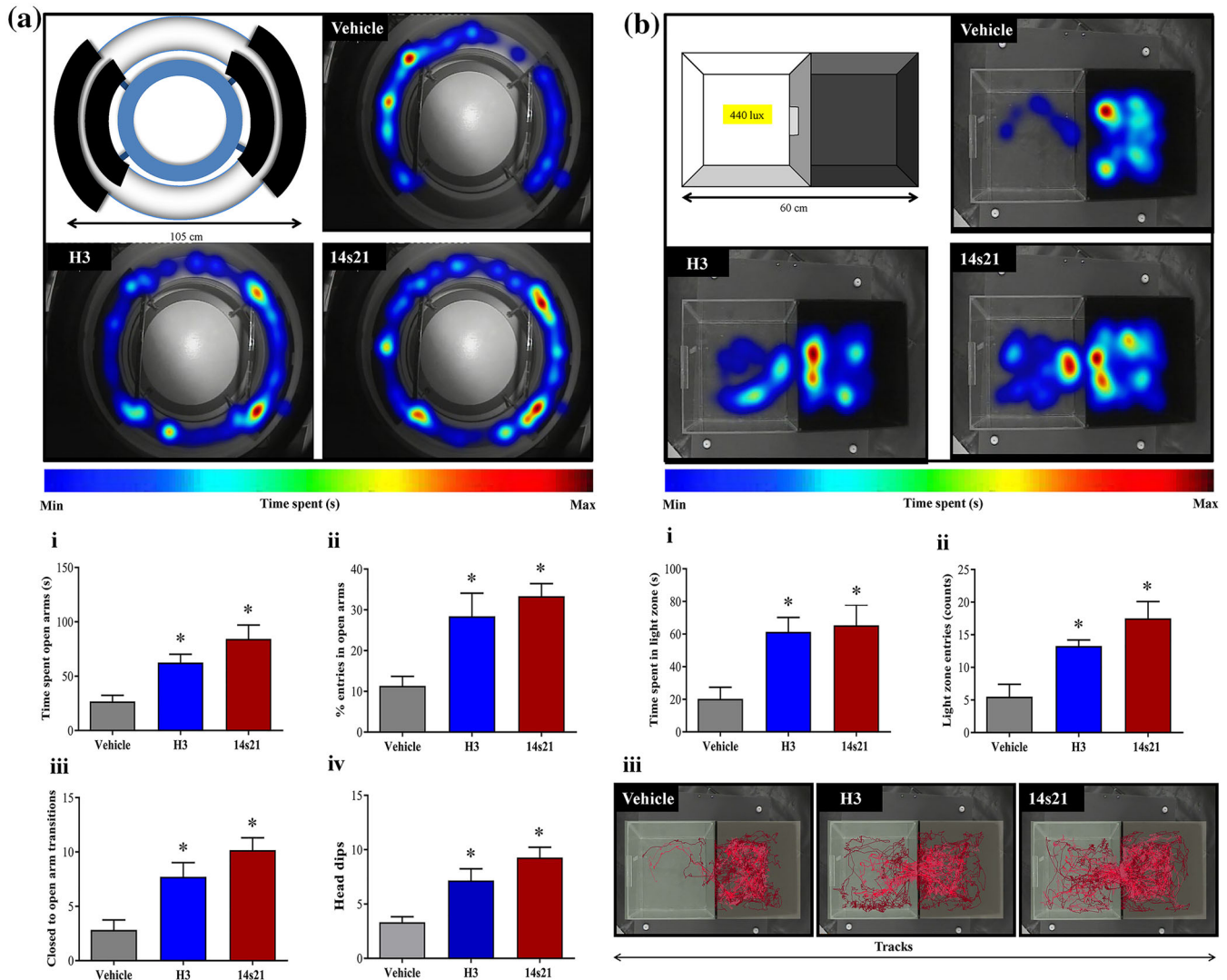


FIGURE 5 Effect of intranasal treatment with H3 relaxin and 14s21 peptide on behaviour in the elevated zero maze (EZM), light-dark box, open field test, and novelty-suppressed feeding test. H3 ($275 \mu\text{g}\cdot\text{kg}^{-1}$) and 14s21 peptide ($1.5 \text{ mg}\cdot\text{kg}^{-1}$) were intranasally administered to rats, and 30 min after drug administration, behaviour was recorded in anxiety behaviour paradigms (a–d). (a) Anxiolytic activity of H3 and the 14s21 peptide in SD rats, indicated by the significantly increased percentage of time spent in the open exposed arms in the EZM (i), total per cent entries made in the open arms (ii), total transitions made from the closed to open arms (iii), and number of head dips over the side while the rat was in the open region (iv). $n = 6$ (vehicle), $n = 7$ (H3), and $n = 6$ (14s21 peptide). (b) The total time spent in the light zone (i) and increased counts in the light zone (ii) indicate the anxiolytic-like effects of H3 and 14s21 peptide in the light/dark exploration test. (iii) Representative activity traces in the LDB for vehicle, H3, and 14s21 peptide. $n = 6$ (vehicle), $n = 7$ (H3), and $n = 6$ (14s21 peptide). (c) In the open field test, both H3- and 14s21 peptide-treated rats showed a significantly increased time spent in the centre of the arena (i), latency to reach to centre (ii), but only the 14s21 peptide displayed a significant increase in velocity, treatment effect: $P < .05$ (iii), but not the total distance travelled (iv), during the experimental paradigm. $n = 7$ (vehicle), $n = 8$ (H3), and $n = 6$ (14s21 peptide). (d) In the novelty-suppressed feeding test, both the H3 relaxin and 14s21 peptide showed a significant time spent in the centre (i), latency to consume the food (ii), and a significant increase in the velocity travelled, (iii), but not in the mean distance travelled in the arena (iv). $n = 7$ (vehicle), $n = 8$ (H3), and $n = 8$ (14s21 peptide). Heat maps representing the time spent in the respective behavioural paradigms (a–d); red = more time and blue = less time. The data in a–d represent the mean \pm SEM. * $P < .05$; significantly different from vehicle; one-way ANOVA followed by Tukey's post hoc multiple comparison

relaxin-3 or RXFP3 receptor agonists consistently induces hyperphagia (Hida et al., 2006; McGowan et al., 2005) and that hypothalamic structures mediate the effects of neuropeptides on food intake (McGowan et al., 2007).

In the EZM and LDB tests, intranasal administration of H3 relaxin and 14s21 peptide produced an anxiolytic effect. We also found a significant effect of H3 relaxin and 14s21 peptide treatment on anxiety-

like measures and locomotor activity in the open field test. Another distinguishing feature of the open field test compared with other approach-avoidance paradigms is the impossibility of “escape” to a safe enclosure, that is, the open field confronts rodents with a novel environment from which there is no escape, while the LDB and EZM provide a safe enclosure (a dark box or closed arms) to which the rodent is able to escape. Locomotor activity was found to be

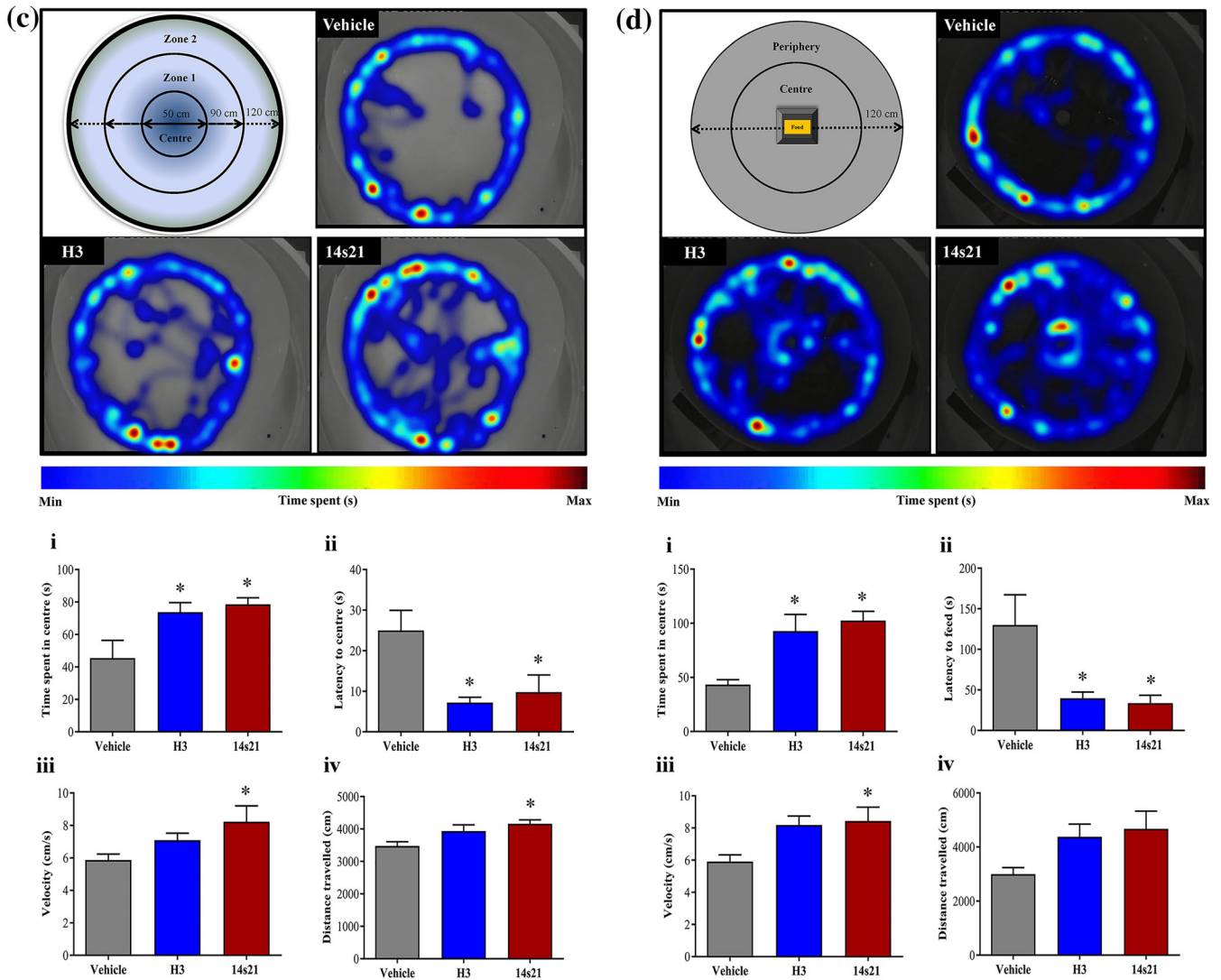


FIGURE 5 Continued.

significantly increased in 14s21-treated animals, which may suggest a role of the relaxin-3/RXFP3 receptor system in preparing behavioural strategies to escape from stressful situations. Similar reductions in anxiety-like behaviour following intracerebroventricular infusion of relaxin-3 in rats were reported previously (Nakazawa et al., 2013; Ryan et al., 2013). These preclinical data suggest that drugs that activate RXFP3 receptors might have potential anxiolytic as well as antidepressant activity. The increased locomotion behaviour along the anxiety profile in the NSFT may be dose dependent and indicates a robust effect, particularly of the 14s21 peptide, suggesting that 14s21 could serve as a potent anxiolytic alternative to benzodiazepines.

Concerning potential antidepressant activity, our data indicated that intranasal treatment with H3 relaxin or 14s21 peptide changed the behavioural strategy used to cope with the stressor more efficiently upon re-exposure to the FST, favouring behavioural activation that could facilitate the anti-immobility effects of antidepressant drugs in the rat FST. Acute or subacute treatment with H3 relaxin or 14s21

peptide did not affect the behavioural score to favour behavioural withdrawal or behavioural despair, as shown by the decreased duration of immobility in the repeat FST; however, chronic treatment with these drugs further increased the immobility compared with the previous exposures. Although both serotonergic and noradrenergic antidepressants reduce the duration of immobility in this test, the selective serotonin reuptake inhibitors (SSRIs) increase “swimming” behaviour, whereas selective noradrenaline reuptake inhibitors (SNRIs) increase “climbing” behaviour. For both H3 relaxin and the 14s21 peptide, the putative SNRI-like climbing behaviour was responsible for most of the total variance in the test, retest 1, and retest 2 analyses.

Relaxin-3 immunoreactive fibres and RXFP3 receptor mRNA are highly concentrated in brain regions involved in stress responses and anxiety-like behaviour, suggesting potential for interactions with 5-HT and CRH signalling in these regions implicated in the aetiology of anxiety and depression (Keck, 2006). Additionally, the effects of RXFP3 receptor activation on eating behaviour highlights the potentially important role of CRH neurons associated with stress signalling

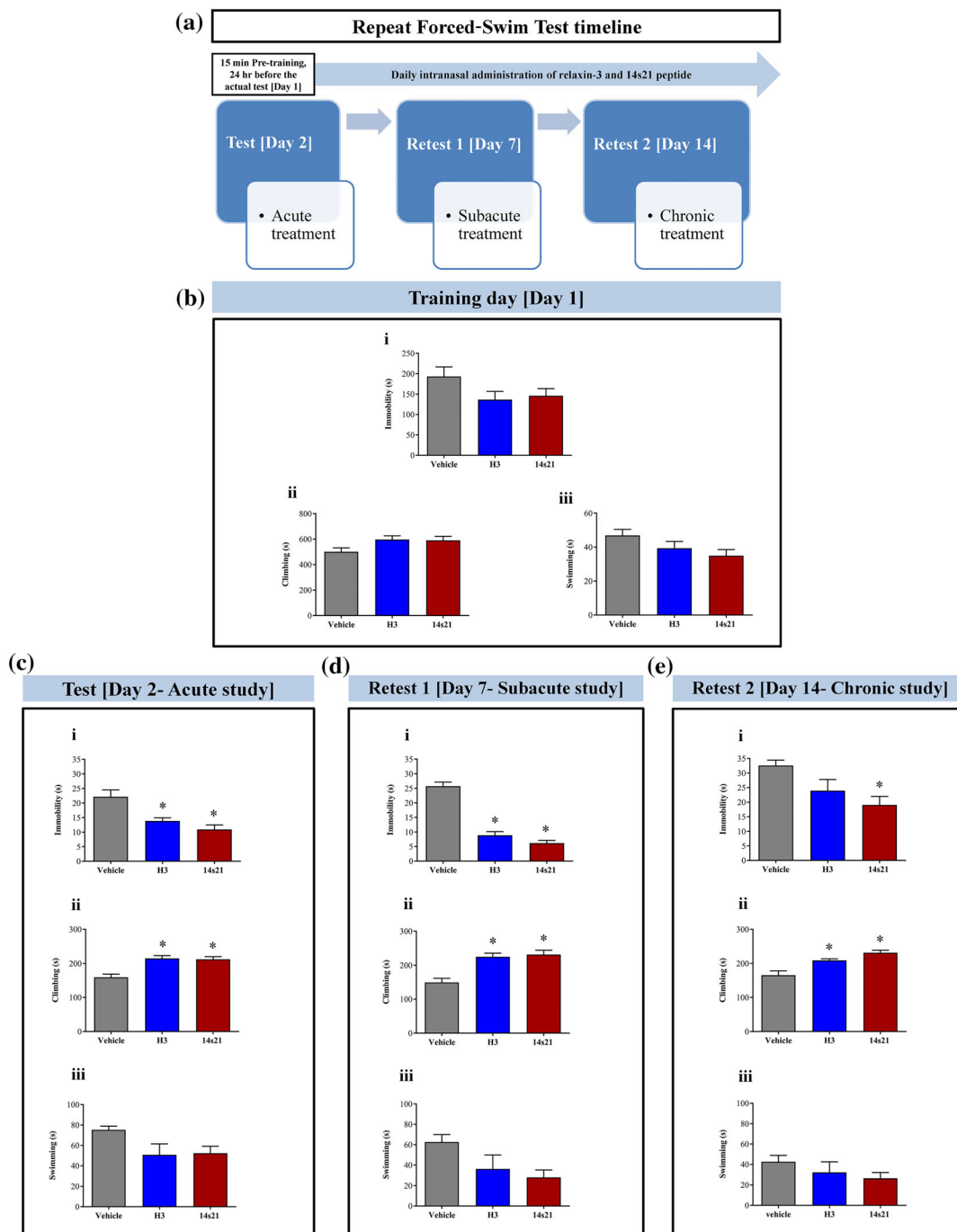


FIGURE 6 Antidepressant activity of H3 relaxin and 14s21 peptide analysed for acute, subacute, and chronic treatment in a repeat forced-swim test (FST). (a) Schematic diagram of the experimental schedule of the repeat FST. Rats were intranasally administered the vehicle, H3 relaxin, or 14s21 peptide, and 30 min after drug administration, behaviour assessment was undertaken in the FST. Twenty-four hours after the pretraining period [training day (Day 1)], rats were intranasally treated with vehicle, H3, or 14s21 peptide to assess behaviour on the actual day of the FST [test (Day 2)]. Daily intranasal administration of vehicle, H3, and 14s21 peptide was then undertaken for 14 days, and the effects of H3 ($275 \mu\text{g}\cdot\text{kg}^{-1}$) and 14s21 peptide ($1.5 \text{ mg}\cdot\text{kg}^{-1}$) intranasal treatment on immobility duration and time spent in climbing and swimming behaviour were recorded for 5 min in female SD rats. (b) Graph showing the results on the first day of treatment and the behaviour analysed during the 15 min of the training period followed by 5-min tests in acute, subacute, and chronic behaviour paradigms. (c) The 5-min test on the next day [test (acute)]. (d) Effects after 7 days of intranasal treatment with vehicle, H3, and 14s21 peptide [retest 1 (subacute)] and (e) 14 days of intranasal administration of vehicle, H3, and 14s21 peptide on immobility, climbing, and swimming behaviour [retest 2 (chronic)]. The bar represents the mean \pm SEM. $n = 6$ rats per group for the vehicle, H3 ($275 \mu\text{g}\cdot\text{kg}^{-1}$), and 14s21 peptide ($1.5 \text{ mg}\cdot\text{kg}^{-1}$) groups. The time spent in immobility significantly decreased over the test and in retest 1, while climbing behaviour significantly increased over the test, retest 1, and retest 2. No significant change in swimming behaviour was observed during the test, retest 1, and retest 2. * $P < .05$, significantly different from vehicle; one-way ANOVA followed by Tukey's post hoc multiple comparison

and the hypothalamic–pituitary–adrenal axis (Carlin, Vale, & Bale, 2006) and the possible actions of oxytocin neurons in feeding behaviour (Blevins, Schwartz, & Baskin, 2004). Considerable evidence supports a role for **oxytocin** in the hypothalamic coordination of metabolic signals (Ganella, Ma, & Gundlach, 2013) and indicates that it is likely to be an effector of relaxin-3/RXFP3 receptor signalling based on the robust expression of these receptors in the hypothalamic nuclei that synthesize oxytocin, the PVN and the SON, and the role of oxytocin in modulating anxiety, fear, and stress responses (Carter, 2003; McCarthy, McDonald, Brooks, & Goldman, 1996; Viero et al., 2010). It was further reported that central infusion of CRH or exposure to neurogenic stressors directly or indirectly activates NI neurons (Ryan, Ma, Olucha-Bordonau, & Gundlach, 2011), and electrolytic lesioning of the NI (Pereira et al., 2013) and selective ablation of **CRF1 receptor**-positive NI neurons using CRH-saporin (Lee, Rajkumar, & Dawe, 2014) cause a deficit in fear conditioning. Moreover, serotonergic afferents are dispersed across multiple regions of the amygdala (Bonn, Schmitt, Lesch, Van Bockstaele, & Asan, 2013), and stress during fear conditioning induces an increase in serotonin concentrations in the amygdala. Thus, SSRIs are used to treat amygdala-related disorders, including anxiety, panic, and phobias (Gorman, 2003). In contrast, catecholaminergic afferents specifically target intercalated nuclei, which are important for conveying information from the prefrontal cortex to the central nucleus, subserving different aspects of extinction memory processing (Quirk, Likhtik, Pelletier, & Pare, 2003). Additionally, noradrenergic projections to the amygdala contribute to reconsolidation of fear memories, and enhancement of noradrenergic neurotransmission impairs extinction of conditioned fear (Debiec, Bush, & LeDoux, 2011). Furthermore, drugs that modify monoaminergic signalling and metabolism have been widely used for many years as treatments for psychiatric disorders, such as anxiety, post-traumatic stress disorders, schizophrenia, and autism (Schumann & Amaral, 2006). Although there is a wealth of data showing multiple types of interactions between noradrenergic and serotonergic neurons (Dale, Bang-Andersen, & Sanchez, 2015), the possibility that H3 relaxin and 14s21 peptide may activate systems other than the serotonergic and noradrenergic systems cannot be excluded. Because both H3 relaxin and 14s21 peptide have been shown to display SSRI-like anxiolytic effects and appear to modulate noradrenergic-like mechanisms underlying antidepressant action, these molecules might exert antidepressant-like effects considering current theories linking anxiety and depression. These profiles of relaxin-3 and 14s21 peptide distinguish them from drugs that primarily activate a single system (i.e., SSRIs or SNRIs) and make them somewhat more similar to dual-acting serotonin/noradrenaline reuptake inhibitors, such as venlafaxine, which are reported to exhibit a faster clinical onset of action and be more effective in treating depression that is refractory to other types of antidepressants.

In conclusion, our the present findings, taken together, suggest that the 14s21 peptide can potentially serve as a useful tool to further probe the importance of the relaxin-3/RXFP3 receptor system in emotional processes and represents a potential novel strategy for the treatment of major depression and anxiety disorders.

ACKNOWLEDGEMENTS

The authors wish to thank Dr Rajkumar Ramamoorthy for expert advice and technical support during in vivo studies and Mr. Ho Woon Fei for excellent technical and administrative assistance.

This work was supported by the NMRC NUHS Centre Grant–Neuroscience Phenotyping Core (Grants NMRC/CG/013/2013 and NMRC/CG/M009/2017_NUH/NUHS) and Ministry of Education, Singapore, Academic Research Fund Tier 1 Grants (T1-BSRG 2014-03 and T1-NUHS O-CRG 2016 Oct-18).

CONFLICT OF INTEREST

S.M. and G.S.D. are co-inventors of an international patent application no. PCT/SG2018/050568 filed on 14 November 2017, entitled “Stapled peptide agonists and their use in treatment of behavioural disorders.”, which is not yet published. The other authors have no conflicts of interest to declare.

AUTHOR CONTRIBUTIONS

S.M. designed, conducted and developed the study, established conditions for in vivo and in vitro experiments, acquired and analysed the data, and wrote the manuscript. A.P. performed the modelling experiments, computational analysis, drew the figures, and contributed to the discussion. N.S. designed the peptide digestion experiments and analysed the results. L.R. supervised circular dichroism, thermal stability experiments, analysed the data, interpreted the results, and contributed to the discussion. C.W.J. and B.W.D. analysed and discussed the data and contributed to the discussion. G.S.D. supervised and conceived the study, designed the in vitro and in vivo experiments, analysed the data, wrote and revised the manuscript with comments from all authors, and provided funding for the study.

DECLARATION OF TRANSPARENCY AND SCIENTIFIC RIGOUR

This Declaration acknowledges that this paper adheres to the principles for transparent reporting and scientific rigour of preclinical research as stated in the *BJP* guidelines for [Design & Analysis, Immunoblotting and Immunochemistry](#), and [Animal Experimentation](#), and as recommended by funding agencies, publishers and other organisations engaged with supporting research.

ORCID

Subhi Marwari  <https://orcid.org/0000-0002-1447-8203>

Gavin Stewart Dawe  <https://orcid.org/0000-0001-6119-701X>

REFERENCES

- Albert-Gasco, H., Garcia-Aviles, A., Moustafa, S., Sanchez-Sarasua, S., Gundlach, A. L., Olucha-Bordonau, F. E., & Sánchez-Pérez, A. M. (2017). Central relaxin-3 receptor (RXFP3) activation increases ERK phosphorylation in septal cholinergic neurons and impairs spatial working memory. *Brain Structure & Function*, 222, 449–463. <https://doi.org/10.1007/s00429-016-1227-8>

- Alexander, S. P. H., Christopoulos, A., Davenport, A. P., Kelly, E., Marrion, N. V., Peters, J. A., ... CGTP Collaborators (2017). The Concise Guide to PHARMACOLOGY 2017/18: G protein-coupled receptors. *British Journal of Pharmacology*, 174(Suppl 1), S17–S129. <https://doi.org/10.1111/bph.13878>
- Alexander, S. P. H., Fabbro, D., Kelly, E., Marrion, N. V., Peters, J. A., Faccenda, E., ... CGTP Collaborators (2017). The Concise Guide to PHARMACOLOGY 2017/18: Enzymes. *British Journal of Pharmacology*, 174, S272–S359. <https://doi.org/10.1111/bph.13877>
- Alexander, S. P. H., Kelly, E., Marrion, N. V., Peters, J. A., Faccenda, E., Harding, S. D., ... CGTP Collaborators (2017). The Concise Guide to PHARMACOLOGY 2017/18: Transporters. *British Journal of Pharmacology*, 174, S360–S446. <https://doi.org/10.1111/bph.13883>
- Bathgate, R. A., Oh, M. H., Ling, W. J., Kaas, Q., Hossain, M. A., Gooley, P. R., & Rosengren, K. J. (2013). Elucidation of relaxin-3 binding interactions in the extracellular loops of RXFP3. *Frontiers in Endocrinology (Lausanne)*, 4, 13.
- Becker, J. B., Prendergast, B. J., & Liang, J. W. (2016). Female rats are not more variable than male rats: A meta-analysis of neuroscience studies. *Biology of Sex Differences*, 7, 34. <https://doi.org/10.1186/s13293-016-0087-5>
- Belzung, C., Yalcin, I., Griebel, G., Surget, A., & Leman, S. (2006). Neuropeptides in psychiatric diseases: An overview with a particular focus on depression and anxiety disorders. *CNS & Neurological Disorders Drug Targets*, 5, 135–145.
- Berridge, C. W., Schmeichel, B. E., & Espana, R. A. (2012). Noradrenergic modulation of wakefulness/arousal. *Sleep Medicine Reviews*, 16, 187–197. <https://doi.org/10.1016/j.smrv.2011.12.003>
- Bird, G. H., Madani, N., Perry, A. F., Princiotto, A. M., Supko, J. G., He, X., ... Walensky, L. D. (2010). Hydrocarbon double-stapling remedies the proteolytic instability of a lengthy peptide therapeutic. *Proceedings of the National Academy of Sciences of the United States of America*, 107, 14093–14098. <https://doi.org/10.1073/pnas.1002713107>
- Blevins, J. E., Schwartz, M. W., & Baskin, D. G. (2004). Evidence that paraventricular nucleus oxytocin neurons link hypothalamic leptin action to caudal brain stem nuclei controlling meal size. *American Journal of Physiology. Regulatory, Integrative and Comparative Physiology*, 287, R87–R96. <https://doi.org/10.1152/ajpregu.00604.2003>
- Bonn, M., Schmitt, A., Lesch, K. P., Van Bockstaele, E. J., & Asan, E. (2013). Serotonergic innervation and serotonin receptor expression of NPY-producing neurons in the rat lateral and basolateral amygdaloid nuclei. *Brain Structure & Function*, 218, 421–435. <https://doi.org/10.1007/s00429-012-0406-5>
- Burazin, T. C., Bathgate, R. A., Macris, M., Layfield, S., Gundlach, A. L., & Tregear, G. W. (2002). Restricted, but abundant, expression of the novel rat gene-3 (R3) relaxin in the dorsal tegmental region of brain. *Journal of Neurochemistry*, 82, 1553–1557. <https://doi.org/10.1046/j.1471-4159.2002.01114.x>
- Caldji, C., Francis, D., Sharma, S., Plotsky, P. M., & Meaney, M. J. (2000). The effects of early rearing environment on the development of GABAA and central benzodiazepine receptor levels and novelty-induced fearfulness in the rat. *Neuropsychopharmacology*, 22, 219–229. [https://doi.org/10.1016/S0893-133X\(99\)00110-4](https://doi.org/10.1016/S0893-133X(99)00110-4)
- Calvez, J., de Avila, C., & Timofeeva, E. (2017). Sex-specific effects of relaxin-3 on food intake and body weight gain. *British Journal of Pharmacology*, 174(10), 1049–1060. <https://doi.org/10.1111/bph.13530>
- Calvez, J., Lenglos, C., de Avila, C., Guevremont, G., & Timofeeva, E. (2015). Differential effects of central administration of relaxin-3 on food intake and hypothalamic neuropeptides in male and female rats. *Genes, Brain, and Behavior*, 14, 550–563. <https://doi.org/10.1111/gbb.12236>
- Carlin, K. M., Vale, W. W., & Bale, T. L. (2006). Vital functions of corticotropin-releasing factor (CRF) pathways in maintenance and regulation of energy homeostasis. *Proceedings of the National Academy of Sciences of the United States of America*, 103, 3462–3467. <https://doi.org/10.1073/pnas.0511320103>
- Carter, C. S. (2003). Developmental consequences of oxytocin. *Physiology & Behavior*, 79, 383–397. [https://doi.org/10.1016/S0031-9384\(03\)00151-3](https://doi.org/10.1016/S0031-9384(03)00151-3)
- Chapuis, H., Slaninova, J., Bednarova, L., Monincova, L., Budesinsky, M., & Cerovsky, V. (2012). Effect of hydrocarbon stapling on the properties of α -helical antimicrobial peptides isolated from the venom of hymenoptera. *Amino Acids*, 43, 2047–2058. <https://doi.org/10.1007/s00726-012-1283-1>
- Crawley, J. N. (1981). Neuropharmacologic specificity of a simple animal model for the behavioral actions of benzodiazepines. *Pharmacology, Biochemistry, and Behavior*, 15, 695–699. [https://doi.org/10.1016/0091-3057\(81\)90007-1](https://doi.org/10.1016/0091-3057(81)90007-1)
- Cromm, P. M., Spiegel, J., & Grossmann, T. N. (2015). Hydrocarbon stapled peptides as modulators of biological function. *ACS Chemical Biology*, 10, 1362–1375. <https://doi.org/10.1021/cb501020r>
- Curtis, M. J., Alexander, S., Cirino, G., Docherty, J. R., George, C. H., Giembycz, M. A., ... Ahluwalia, A. (2018). Experimental design and analysis and their reporting II: Updated and simplified guidance for authors and peer reviewers. *British Journal of Pharmacology*, 175, 987–993. <https://doi.org/10.1111/bph.14153>
- Dale, E., Bang-Andersen, B., & Sanchez, C. (2015). Emerging mechanisms and treatments for depression beyond SSRIs and SNRIs. *Biochemical Pharmacology*, 95, 81–97. <https://doi.org/10.1016/j.bcp.2015.03.011>
- Debiec, J., Bush, D. E., & LeDoux, J. E. (2011). Noradrenergic enhancement of reconsolidation in the amygdala impairs extinction of conditioned fear in rats—A possible mechanism for the persistence of traumatic memories in PTSD. *Depression and Anxiety*, 28, 186–193. <https://doi.org/10.1002/da.20803>
- Derkach, K. V., Bondareva, V. M., Chistyakova, O. V., Berstein, L. M., & Shpakov, A. O. (2015). The effect of long-term intranasal serotonin treatment on metabolic parameters and hormonal signaling in rats with high-fat diet/low-dose streptozotocin-induced type 2 diabetes. *International Journal of Endocrinology*, 2015, 245459.
- Dhuria, S. V., Hanson, L. R., & Frey, W. H. 2nd (2009). Intranasal drug targeting of hypocretin-1 (orexin-A) to the central nervous system. *Journal of Pharmaceutical Sciences*, 98, 2501–2515. <https://doi.org/10.1002/jps.21604>
- Ganella, D. E., Ma, S., & Gundlach, A. L. (2013). Relaxin-3/RXFP3 signaling and neuroendocrine function—A perspective on extrinsic hypothalamic control. *Frontiers in Endocrinology (Lausanne)*, 4, 128.
- Ganella, D. E., Ryan, P. J., Bathgate, R. A., & Gundlach, A. L. (2012). Increased feeding and body weight gain in rats after acute and chronic activation of RXFP3 by relaxin-3 and receptor-selective peptides: Functional and therapeutic implications. *Behavioural Pharmacology*, 23, 516–525. <https://doi.org/10.1097/FBP.0b013e3283576999>
- Gorman, J. M. (2003). Treating generalized anxiety disorder. *The Journal of Clinical Psychiatry*, 64(Suppl 2), 24–29.
- Grivas, V., Markou, A., & Pitsikas, N. (2013). The metabotropic glutamate 2/3 receptor agonist LY379268 induces anxiety-like behavior at the highest dose tested in two rat models of anxiety. *European Journal of Pharmacology*, 715, 105–110. <https://doi.org/10.1016/j.ejphar.2013.05.048>
- Grupe, D. W., & Nitschke, J. B. (2013). Uncertainty and anticipation in anxiety: An integrated neurobiological and psychological perspective. *Nature Reviews. Neuroscience*, 14, 488–501. <https://doi.org/10.1038/nrn3524>

- Guo, Z., Mohanty, U., Noehre, J., Sawyer, T. K., Sherman, W., & Krilov, G. (2010). Probing the α -helical structural stability of stapled p53 peptides: Molecular dynamics simulations and analysis. *Chemical Biology & Drug Design*, 75, 348–359. <https://doi.org/10.1111/j.1747-0285.2010.00951.x>
- Hallschmid, M., Benedict, C., Schultes, B., Perras, B., Fehm, H. L., Kern, W., & Born, J. (2008). Towards the therapeutic use of intranasal neuropeptide administration in metabolic and cognitive disorders. *Regulatory Peptides*, 149, 79–83. <https://doi.org/10.1016/j.regpep.2007.06.012>
- Harding, S. D., Sharman, J. L., Faccenda, E., Southan, C., Pawson, A. J., Ireland, S., ... NC-IUPHAR (2018). The IUPHAR/BPS guide to PHARMACOLOGY in 2018: Updates and expansion to encompass the new guide to IMMUNOPHARMACOLOGY. *Nucleic Acids Research*, 46, D1091–D1106. <https://doi.org/10.1093/nar/gkx1121>
- Harris, G. L., Creason, M. B., Brulte, G. B., & Herr, D. R. (2012). In vitro and in vivo antagonism of a G protein-coupled receptor (S1P3) with a novel blocking monoclonal antibody. *PLoS ONE*, 7, e35129. <https://doi.org/10.1371/journal.pone.0035129>
- Haugaard-Kedstrom, L. M., Wong, L. L., Bathgate, R. A., & Rosengren, K. J. (2015). Synthesis and pharmacological characterization of a europium-labelled single-chain antagonist for binding studies of the relaxin-3 receptor RXFP3. *Amino Acids*, 47, 1267–1271. <https://doi.org/10.1007/s00726-015-1961-x>
- Hida, T., Takahashi, E., Shikata, K., Hirohashi, T., Sawai, T., Seiki, T., ... Kuromitsu, J. (2006). Chronic intracerebroventricular administration of relaxin-3 increases body weight in rats. *Journal of Receptor and Signal Transduction Research*, 26, 147–158. <https://doi.org/10.1080/10799890600623373>
- Hojo, K., Hossain, M. A., Tailhades, J., Shabanpoor, F., Wong, L. L., Ong-Palsson, E. E., ... Bathgate, R. A. (2016). Development of a single-chain peptide agonist of the relaxin-3 receptor using hydrocarbon stapling. *Journal of Medicinal Chemistry*, 59, 7445–7456. <https://doi.org/10.1021/acs.jmedchem.6b00265>
- Hu, M. J., Shao, X. X., Wang, J. H., Wei, D., Liu, Y. L., Xu, Z. G., & Guo, Z. Y. (2016). Identification of hydrophobic interactions between relaxin-3 and its receptor RXFP3: Implication for a conformational change in the B-chain C-terminus during receptor binding. *Amino Acids*, 48, 2227–2236. <https://doi.org/10.1007/s00726-016-2260-x>
- Ionescu, I. A., Dine, J., Yen, Y. C., Buell, D. R., Herrmann, L., Holsboer, F., ... Schmidt, U. (2012). Intranasally administered neuropeptide S (NPS) exerts anxiolytic effects following internalization into NPS receptor-expressing neurons. *Neuropsychopharmacology*, 37, 1323–1337. <https://doi.org/10.1038/npp.2011.317>
- Jayakody, T., Marwari, S., Lakshminarayanan, R., Tan, F. C., Johannes, C. W., Dymock, B. W., ... Dawe, G. S. (2016). Hydrocarbon stapled B chain analogues of relaxin-3 retain biological activity. *Peptides*, 84, 44–57. <https://doi.org/10.1016/j.peptides.2016.08.001>
- Kania, A., Gugula, A., Grabowiecka, A., de Avila, C., Blasiak, T., Rajfur, Z., ... Blasiak, A. (2017). Inhibition of oxytocin and vasopressin neuron activity in rat hypothalamic paraventricular nucleus by relaxin-3-RXFP3 signalling. *The Journal of Physiology*, 595, 3425–3447. <https://doi.org/10.1113/JP273787>
- Keck, M. E. (2006). Corticotropin-releasing factor, vasopressin and receptor systems in depression and anxiety. *Amino Acids*, 31, 241–250. <https://doi.org/10.1007/s00726-006-0333-y>
- Kessler, R. C., Aguilar-Gaxiola, S., Alonso, J., Chatterji, S., Lee, S., Ormel, J., ... Wang, P. S. (2009). The global burden of mental disorders: An update from the WHO World Mental Health (WMH) surveys. *Epidemiologia e Psichiatria Sociale*, 18, 23–33. <https://doi.org/10.1017/S1121189X00001421>
- Kilkenny, C., Browne, W., Cuthill, I. C., Emerson, M., & Altman, D. G. (2010). Animal research: Reporting in vivo experiments: The ARRIVE guidelines. *British Journal of Pharmacology*, 160, 1577–1579.
- Kuei, C., Sutton, S., Bonaventure, P., Pudiak, C., Shelton, J., Zhu, J., ... Liu, C. (2007). R3(B Δ 23 27)R/I5 chimeric peptide, a selective antagonist for GPCR135 and GPCR142 over relaxin receptor LGR7: In vitro and in vivo characterization. *The Journal of Biological Chemistry*, 282, 25425–25435. <https://doi.org/10.1074/jbc.M701416200>
- Kumar, J. R., Rajkumar, R., Farooq, U., Lee, L. C., Tan, F. C., & Dawe, G. S. (2015). Evidence of D2 receptor expression in the nucleus incertus of the rat. *Physiology & Behavior*, 151, 525–534. <https://doi.org/10.1016/j.physbeh.2015.08.024>
- Kumar, J. R., Rajkumar, R., Jayakody, T., Marwari, S., Hong, J. M., Ma, S., ... Dawe, G. S. (2017). Relaxin' the brain: A case for targeting the nucleus incertus network and relaxin-3/RXFP3 system in neuropsychiatric disorders. *British Journal of Pharmacology*, 174, 1061–1076. <https://doi.org/10.1111/bph.13564>
- Kumar, N. N., Lochhead, J. J., Pizzo, M. E., Nehra, G., Boroumand, S., Greene, G., & Thorne, R. G. (2018). Delivery of immunoglobulin G antibodies to the rat nervous system following intranasal administration: Distribution, dose-response, and mechanisms of delivery. *Journal of Controlled Release*, 286, 467–484. <https://doi.org/10.1016/j.jconrel.2018.08.006>
- Lee, L. C., Rajkumar, R., & Dawe, G. S. (2014). Selective lesioning of nucleus incertus with corticotropin releasing factor-saporin conjugate. *Brain Research*, 1543, 179–190. <https://doi.org/10.1016/j.brainres.2013.11.021>
- Lesch, K. P., & Waider, J. (2012). Serotonin in the modulation of neural plasticity and networks: Implications for neurodevelopmental disorders. *Neuron*, 76, 175–191. <https://doi.org/10.1016/j.neuron.2012.09.013>
- Lezak, K. R., Missig, G., & Carlezon, W. A. Jr. (2017). Behavioral methods to study anxiety in rodents. *Dialogues in Clinical Neuroscience*, 19, 181–191.
- Lino-de-Oliveira, C., De Lima, T. C., & de Padua Carobrez, A. (2005). Structure of the rat behaviour in the forced swimming test. *Behavioural Brain Research*, 158, 243–250. <https://doi.org/10.1016/j.bbr.2004.09.004>
- Liu, C., Eriste, E., Sutton, S., Chen, J., Roland, B., Kuei, C., ... Lovenberg, T. W. (2003). Identification of relaxin-3/INSL7 as an endogenous ligand for the orphan G-protein-coupled receptor GPCR135. *The Journal of Biological Chemistry*, 278, 50754–50764. <https://doi.org/10.1074/jbc.M308995200>
- Lukas, M., & Neumann, I. D. (2012). Nasal application of neuropeptide S reduces anxiety and prolongs memory in rats: Social versus non-social effects. *Neuropharmacology*, 62, 398–405. <https://doi.org/10.1016/j.neuropharm.2011.08.016>
- Ma, S., Bonaventure, P., Ferraro, T., Shen, P. J., Burazin, T. C., Bathgate, R. A., ... Gundlach, A. L. (2007). Relaxin-3 in GABA projection neurons of nucleus incertus suggests widespread influence on forebrain circuits via G-protein-coupled receptor-135 in the rat. *Neuroscience*, 144, 165–190. <https://doi.org/10.1016/j.neuroscience.2006.08.072>
- Ma, S., Sang, Q., Lanciego, J. L., & Gundlach, A. L. (2009). Localization of relaxin-3 in brain of *Macaca fascicularis*: Identification of a nucleus incertus in primate. *The Journal of Comparative Neurology*, 517, 856–872. <https://doi.org/10.1002/cne.22197>
- Ma, S., Smith, C. M., Blasiak, A., & Gundlach, A. L. (2017). Distribution, physiology and pharmacology of relaxin-3/RXFP3 systems in brain. *British Journal of Pharmacology*, 174, 1034–1048. <https://doi.org/10.1111/bph.13659>
- Matsumoto, M., Kamohara, M., Sugimoto, T., Hidaka, K., Takasaki, J., Saito, T., ... Furuichi, K. (2000). The novel G-protein coupled receptor SALPR

- shares sequence similarity with somatostatin and angiotensin receptors. *Gene*, 248, 183–189. [https://doi.org/10.1016/S0378-1119\(00\)00123-2](https://doi.org/10.1016/S0378-1119(00)00123-2)
- McCarthy, M. M., McDonald, C. H., Brooks, P. J., & Goldman, D. (1996). An anxiolytic action of oxytocin is enhanced by estrogen in the mouse. *Physiology & Behavior*, 60, 1209–1215. [https://doi.org/10.1016/S0031-9384\(96\)00212-0](https://doi.org/10.1016/S0031-9384(96)00212-0)
- McGowan, B. M., Stanley, S. A., Smith, K. L., Minnion, J. S., Donovan, J., Thompson, E. L., ... Bloom, S. R. (2006). Effects of acute and chronic relaxin-3 on food intake and energy expenditure in rats. *Regulatory Peptides*, 136, 72–77. <https://doi.org/10.1016/j.regpep.2006.04.009>
- McGowan, B. M., Stanley, S. A., Smith, K. L., White, N. E., Connolly, M. M., Thompson, E. L., ... Bloom, S. R. (2005). Central relaxin-3 administration causes hyperphagia in male Wistar rats. *Endocrinology*, 146, 3295–3300. <https://doi.org/10.1210/en.2004-1532>
- McGowan, B. M., Stanley, S. A., White, N. E., Spangeus, A., Patterson, M., Thompson, E. L., ... Bloom, S. R. (2007). Hypothalamic mapping of orexigenic action and Fos-like immunoreactivity following relaxin-3 administration in male Wistar rats. *American Journal of Physiology. Endocrinology and Metabolism*, 292, E913–E919. <https://doi.org/10.1152/ajpendo.00346.2006>
- Mezadri, T. J., Batista, G. M., Portes, A. C., Marino-Neto, J., & Lino-de-Oliveira, C. (2011). Repeated rat-forced swim test: Reducing the number of animals to evaluate gradual effects of antidepressants. *Journal of Neuroscience Methods*, 195, 200–205. <https://doi.org/10.1016/j.jneumeth.2010.12.015>
- Migliore, M. M., Ortiz, R., Dye, S., Campbell, R. B., Amiji, M. M., & Waszczak, B. L. (2014). Neurotrophic and neuroprotective efficacy of intranasal GDNF in a rat model of Parkinson's disease. *Neuroscience*, 274, 11–23. <https://doi.org/10.1016/j.neuroscience.2014.05.019>
- Monti, J. M., & Jantos, H. (2008). The roles of dopamine and serotonin, and of their receptors, in regulating sleep and waking. *Progress in Brain Research*, 172, 625–646. [https://doi.org/10.1016/S0079-6123\(08\)00929-1](https://doi.org/10.1016/S0079-6123(08)00929-1)
- Nakazawa, C. M., Shikata, K., Uesugi, M., Katayama, H., Aoshima, K., Tahara, K., ... Miyamoto, N. (2013). Prediction of relaxin-3-induced downstream pathway resulting in anxiolytic-like behaviors in rats based on a microarray and peptidome analysis. *Journal of Receptor and Signal Transduction Research*, 33, 224–233. <https://doi.org/10.3109/10799893.2012.756895>
- Olucha-Bordonau, F. E., Otero-Garcia, M., Sanchez-Perez, A. M., Nunez, A., Ma, S., & Gundlach, A. L. (2012). Distribution and targets of the relaxin-3 innervation of the septal area in the rat. *The Journal of Comparative Neurology*, 520, 1903–1939. <https://doi.org/10.1002/cne.23018>
- Otsubo, H., Onaka, T., Suzuki, H., Katoh, A., Ohbuchi, T., Todoroki, M., ... Ueta, Y. (2010). Centrally administered relaxin-3 induces Fos expression in the osmosensitive areas in rat brain and facilitates water intake. *Peptides*, 31, 1124–1130. <https://doi.org/10.1016/j.peptides.2010.02.020>
- Paxinos, G., & Watson, C. (2007). *The rat brain in stereotaxic coordinates* (6th ed.). London: Academic Press.
- Pereira, C. W., Santos, F. N., Sanchez-Perez, A. M., Otero-Garcia, M., Marchioro, M., Ma, S., ... Olucha-Bordonau, F. E. (2013). Electrolytic lesion of the nucleus incertus retards extinction of auditory conditioned fear. *Behavioural Brain Research*, 247, 201–210. <https://doi.org/10.1016/j.bbr.2013.03.025>
- Pollak, D. D., Rey, C. E., & Monje, F. J. (2010). Rodent models in depression research: Classical strategies and new directions. *Annals of Medicine*, 42, 252–264. <https://doi.org/10.3109/07853891003769957>
- Quirk, G. J., Likhtik, E., Pelletier, J. G., & Pare, D. (2003). Stimulation of medial prefrontal cortex decreases the responsiveness of central amygdala output neurons. *The Journal of Neuroscience*, 23, 8800–8807. <https://doi.org/10.1523/JNEUROSCI.23-25-08800.2003>
- Rosengren, K. J., Lin, F., Bathgate, R. A., Tregear, G. W., Daly, N. L., Wade, J. D., & Craik, D. J. (2006). Solution structure and novel insights into the determinants of the receptor specificity of human relaxin-3. *The Journal of Biological Chemistry*, 281, 5845–5851. <https://doi.org/10.1074/jbc.M511210200>
- Ryan, P. J., Buchler, E., Shabanpoor, F., Hossain, M. A., Wade, J. D., Lawrence, A. J., & Gundlach, A. L. (2013). Central relaxin-3 receptor (RXFP3) activation decreases anxiety- and depressive-like behaviours in the rat. *Behavioural Brain Research*, 244, 142–151. <https://doi.org/10.1016/j.bbr.2013.01.034>
- Ryan, P. J., Ma, S., Olucha-Bordonau, F. E., & Gundlach, A. L. (2011). Nucleus incertus—An emerging modulatory role in arousal, stress and memory. *Neuroscience and Biobehavioral Reviews*, 35, 1326–1341. <https://doi.org/10.1016/j.neubiorev.2011.02.004>
- Schumann, C. M., & Amaral, D. G. (2006). Stereological analysis of amygdala neuron number in autism. *The Journal of Neuroscience*, 26, 7674–7679. <https://doi.org/10.1523/JNEUROSCI.1285-06.2006>
- Shaul, Y., & Seger, R. (2006). The detection of MAPK signaling. *Current Protocols in Molecular Biology*. Chapter 18: Unit 18 12
- Shepherd, J. K., Grewal, S. S., Fletcher, A., Bill, D. J., & Dourish, C. T. (1994). Behavioural and pharmacological characterisation of the elevated “zero-maze” as an animal model of anxiety. *Psychopharmacology*, 116, 56–64. <https://doi.org/10.1007/BF02244871>
- Smith, C. M., Shen, P. J., Banerjee, A., Bonaventure, P., Ma, S., Bathgate, R. A., ... Gundlach, A. L. (2010). Distribution of relaxin-3 and RXFP3 within arousal, stress, affective, and cognitive circuits of mouse brain. *The Journal of Comparative Neurology*, 518, 4016–4045. <https://doi.org/10.1002/cne.22442>
- Takagi, H., Shiosaka, S., Tohyama, M., Senba, E., & Sakanaka, M. (1980). Ascending components of the medial forebrain bundle from the lower brain stem in the rat, with special reference to raphe and catecholamine cell groups. A study by the HRP method. *Brain Research*, 193, 315–337. [https://doi.org/10.1016/0006-8993\(80\)90168-7](https://doi.org/10.1016/0006-8993(80)90168-7)
- Tanaka, M., Iijima, N., Miyamoto, Y., Fukusumi, S., Itoh, Y., Ozawa, H., & Ibata, Y. (2005). Neurons expressing relaxin 3/INSL 7 in the nucleus incertus respond to stress. *The European Journal of Neuroscience*, 21, 1659–1670. <https://doi.org/10.1111/j.1460-9568.2005.03980.x>
- Thorne, R. G., Pronk, G. J., Padmanabhan, V., & Frey, W. H. 2nd (2004). Delivery of insulin-like growth factor-I to the rat brain and spinal cord along olfactory and trigeminal pathways following intranasal administration. *Neuroscience*, 127, 481–496. <https://doi.org/10.1016/j.neuroscience.2004.05.029>
- van der Westhuizen, E. T., Werry, T. D., Sexton, P. M., & Summers, R. J. (2007). The relaxin family peptide receptor 3 activates extracellular signal-regulated kinase 1/2 through a protein kinase C-dependent mechanism. *Molecular Pharmacology*, 71, 1618–1629. <https://doi.org/10.1124/mol.106.032763>
- Viero, C., Shibuya, I., Kitamura, N., Verkhatsky, A., Fujihara, H., Katoh, A., ... Dayanithi, G. (2010). REVIEW: Oxytocin: Crossing the bridge between basic science and pharmacotherapy. *CNS Neuroscience & Therapeutics*, 16, e138–e156. <https://doi.org/10.1111/j.1755-5949.2010.00185.x>
- Walensky, L. D., & Bird, G. H. (2014). Hydrocarbon-stapled peptides: Principles, practice, and progress. *Journal of Medicinal Chemistry*, 57, 6275–6288. <https://doi.org/10.1021/jm4011675>
- Walensky, L. D., Kung, A. L., Escher, I., Malia, T. J., Barbuto, S., Wright, R. D., ... Korsmeyer, S. J. (2004). Activation of apoptosis in vivo by a hydrocarbon-stapled BH3 helix. *Science*, 305, 1466–1470. <https://doi.org/10.1126/science.1099191>

- Wang, P. S., & Insel, T. R. (2010). NIMH-funded pragmatic trials: Moving on. *Neuropsychopharmacology*, 35, 2489–2490. <https://doi.org/10.1038/npp.2010.161>
- Watanabe, Y., Miyamoto, Y., Matsuda, T., & Tanaka, M. (2011). Relaxin-3/INSL7 regulates the stress-response system in the rat hypothalamus. *Journal of Molecular Neuroscience*, 43, 169–174. <https://doi.org/10.1007/s12031-010-9468-0>
- Whiteford, H. A., & Baxter, A. J. (2013). The Global Burden of Disease 2010 Study: What does it tell us about mental disorders in Latin America? *Revista Brasileira de Psiquiatria*, 35, 111–112. <https://doi.org/10.1590/1516-4446-2012-3502>
- Whiteford, H. A., Degenhardt, L., Rehm, J., Baxter, A. J., Ferrari, A. J., Erskine, H. E., ... Vos, T. (2013). Global burden of disease attributable to mental and substance use disorders: Findings from the Global Burden of Disease Study 2010. *Lancet*, 382, 1575–1586. [https://doi.org/10.1016/S0140-6736\(13\)61611-6](https://doi.org/10.1016/S0140-6736(13)61611-6)

- Wong, L. L. L., Scott, D. J., Hossain, M. A., Kaas, Q., Rosengren, K. J., & Bathgate, R. A. D. (2018). Distinct but overlapping binding sites of agonist and antagonist at the relaxin family peptide 3 (RXFP3) receptor. *The Journal of Biological Chemistry*, 293, 15777–15789. <https://doi.org/10.1074/jbc.RA118.002645>

SUPPORTING INFORMATION

Additional supporting information may be found online in the Supporting Information section at the end of the article.

How to cite this article: Marwari S, Poulsen A, Shih N, et al. Intranasal administration of a stapled relaxin-3 mimetic has anxiolytic- and antidepressant-like activity in rats. *Br J Pharmacol*. 2019;176:3899–3923. <https://doi.org/10.1111/bph.14774>